UNIVERSITY OF CALIFORNIA
SANTA CRUZ

Noise Studies on Silicon Microstrip Detectors

A thesis submitted in partial satisfaction
of the requirements of the degree of

BACHELOR OF SCIENCE

in

PHYSICS

by

Teela Marie Pulliam

18 June 1995

This thesis of Teela Marie Pulliam is approved by:

Hartmut Sadrozinski
Technical Advisor

George Brown
Thesis Advisor
1994-1995

David E. Dorfan
Chair, Board of Physics

Table of Contents

List of Figures

List of Tables

Abstract

Silicon microstrip detectors are examined with an emphasis on noise measurement. Two different noise measurement methods; the calibration and occupancy method, are presented and compared. Both are found to yield accurate results. Noise is measured for different strip lengths and configurations which are compared in order to examine how noise scales with length and capacitance.

Acknowledgments

I would like to thank Hartmut Sadrozinski for providing excitement and guidance in this project. I also would like to offer a special thanks to Bill Rowe for his miracle bonding and all around help and support. A big thank you to Tim Dubbs, Wilko Kröger and Max Wilder for listening to all my questions and explaining over and over again. Thanks to Alec Webster for all the support and advice and to Alex Grillo for lending me your pen again and again.

Warm thanks the members of TT an organization I would not have made it without; Scott Plette and especially Jason Patton for being my faithful lab partner on every occasion.

Lavish thanks to David for doing all the dishes while I was working on my thesis. And last but not least thanks to my parents for all of their love, encouragement and financial support not only through the last four years but from the very beginning.

I. INTRODUCTION

Experiments in high energy physics involve the observation of particles and their interactions. Many of these experiments involve collider systems, where beams of particles are accelerated to high energies and forced to interact. When particles collide they break apart or combine together to form other particles. In this way physicists probe the structure of the matter or create particles that would not usually exist in the universe today.

The interaction area [figure 1], where the beams of particles collide, is surrounded by detectors designed to measure various properties of the interaction.

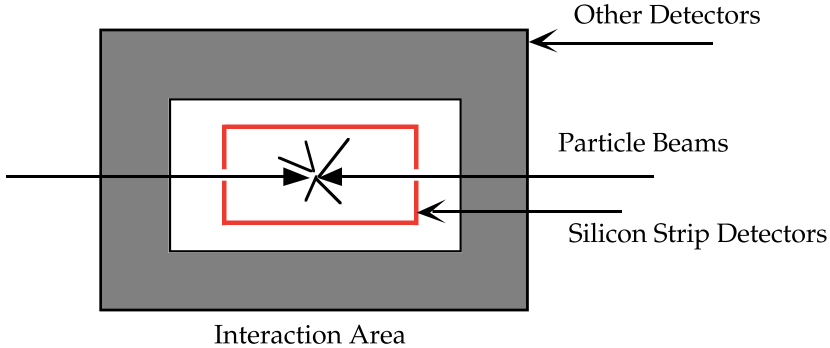

Figure 1 - Interaction area of a colliding particle experiment.

Properties of the particles such as energy, position and momentum are measured using many different types of detectors. The innermost layer of detectors in most collider experiments consists of silicon strip detectors which provide a precise measurement of the position of the particles. These are surrounded by other detectors which measure properties such as the energy of the particles [calorimeters] or the trajectory further away from the collision point [drift chambers].

I will examine silicon micro-strip detectors. In particular, I will explore the noise characterization of these detectors for different lengths and configurations. I will also examine and compare two different methods of measuring the noise.

I start out with a background section that describes how the detectors are used, how they work and defines the noise that was measured. In my materials and methods section I give a description of the apparatus that was used to make the measurements and the two methods used to measure noise.

The results and discussion section presents the results for different detector lengths and configurations. In the conclusion I discuss future measurements that will be made to continue this examination.

The detector and experimental set up used for the measurements presented here were designed for use in a test beam at KEK in Japan. They were manufactured for design research and development; not to be used in a physics experiment.

II. BACKGROUND

Silicon Microstrip Detectors

Silicon microstrip detectors are a relatively new development in particle detection. They can determine the position of a particle to within 10 microns or less which is 10 times better precision than with older detectors such as wire chambers[1].

Silicon strip detectors use diodes to detect particles. A diode is a device that allows current to flow in only one direction. This ability to block current flow is the reason to use diodes as a measurement device; otherwise, the faint signals caused by particles can be lost in statistical fluctuations in the current.

Silicon strip detectors are manufactured by implanting strips of doped silicon into a silicon crystal wafer. The implants can be positively or negatively doped. This is done by adding a very small number of impurity atoms to pure silicon crystal. Silicon crystal has a diamondlike structure: every atom has four equidistant neighbors and shares one of its four outer electrons with each neighbor[2]. By adding impurity atoms with different numbers of outer electrons, doped silicon can be produced that has an excess of negative or positive charge carriers. For example, adding a small number of phosphorus atoms, which have five outer electrons, will result in an excess of negative charge carriers since the fifth outer electron will not be bound to a neighbor and can be easily liberated to carry an electronic current. This kind of doping is called n-type since the resulting material has excess negative charge carriers. Silicon can also be doped with an atom that has only three outer electrons, such as boron. This results in a empty space where an

[1] Litke and Schwarz, p. 77.
[2] ibid.

electron wants to be, or a "hole" in the crystal, which functions as a positive charge carrier. Positively doped silicon is dubbed p-type.

Diodes are formed by a junction of p and n-type silicon. At the junction area the negative carriers [electrons] from the n-type silicon can diffuse into the p-type silicon and be neutralized by the positive carriers [holes], leaving behind ionized impurity atoms on either side of the junction[3]. These ionized atoms create an electric field which keep holes on the p-side and electrons on the n-side of the junction. This creates a region around the junction which is free of charge carriers and has a strong electric field. This region is called the depletion region and can be expanded by placing a voltage with the proper polarity on either side of the diode junction. A positive voltage is placed on the n-type implant and negative carriers are attracted out of the implant, conversely a negative voltage is placed on the p-type implant to attract positive carriers. The depleted region acts as the particle detector.

A double sided silicon strip detector has implants on both sides. One side, the n-side, has n-type implants while the other, the p-side, has p-type implants.

When a particle passes through the detector it liberates electron-hole pairs [figure 2].

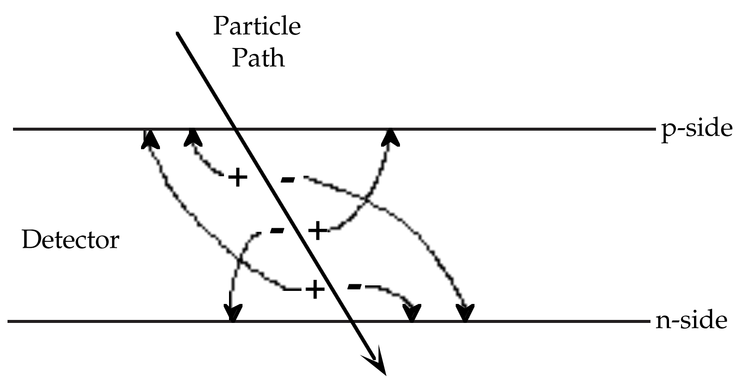

Figure 2 - Particle passing through detector.

The holes [represented by '+' in figure 2] are attracted to the p-side by the negative bias voltage, and the electrons [represented by '-' in figure 2] are attracted to the n-side by the positive bias voltage. This signal is then

3 ibid.

amplified and recorded by electronic readout chips located next to the detector.

A double sided silicon strip detector is shown in figure 3.

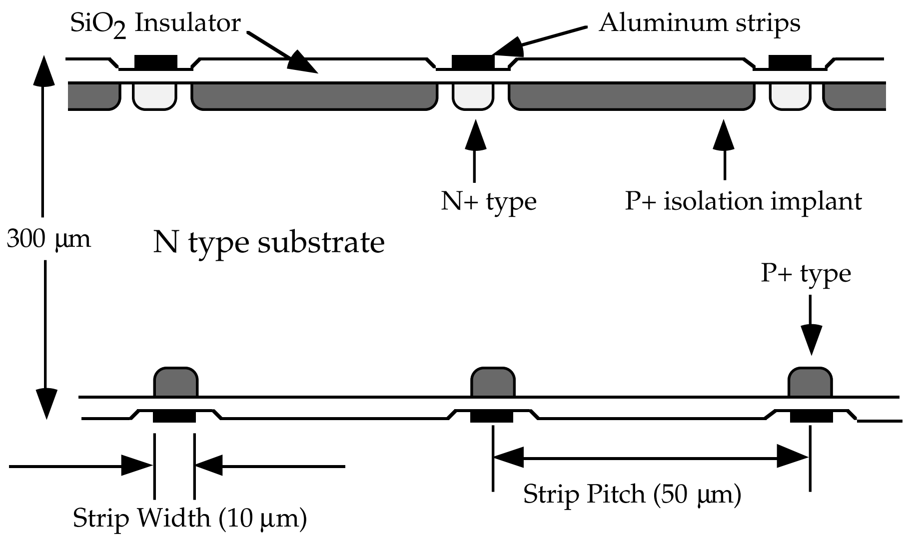

Figure 3 - Double sided silicon strip detector cross-section.[4]

The substrate, or bulk of the detector, is n-type. On the n-side the implants are of type n+ [highly doped n-type silicon], which are isolated from each other by p+ [highly doped p-type silicon] isolation implants in-between the strips. On the p-side the strips are p+ implants and isolation implants are not needed since the substrate is n-type. The junction between the p+ implants and the n-type substrate is where the diode is formed. Aluminum strips on top of the implants serve to carry the signal to the readout electronics. For AC coupled detectors there is a thin insulating layer of silicon oxide in-between the implants and the aluminum strips. The implants and the metal strips above them form a 15pF/cm coupling capacitor through which the signal travels.

Noise

The signal caused by a particle[5] can easily be affected by noise generated by the detector or the electronics used to record it. Therefore, in order to understand the signal to noise ratio the noise of the system must be characterized.

---

[4] Drawing by John Nibarger, SCIPP, UCSC, 1995.
[5] The signal caused by one minimum ionizing particle is around 4fC.

A simple approximation can be made for the noise charge which only takes into consideration the contribution from the electronics and the capacitance of the strip being measured:

$$\text{Noise} = A + BC \qquad [1]$$

A is the constant noise contribution from the electronics with out the strip connected. B is a constant factor that has been found[6] to be around 32 e^-/pF, and C is the capacitance of the strip.

In reality, there are other contributions to the noise. There is a contribution from the electronics that the neighboring strips are connected to and from the resistance of the measured strip. There also is a contribution to the noise from the bias [leakage] current[7]. By comparing theoretical values for the noise, obtained from equation 1, with actual measurements one can determine the magnitude of the other contributions.

III. MATERIALS AND METHOD:

Experimental Set Up

The experimental set up is shown in figure 4.

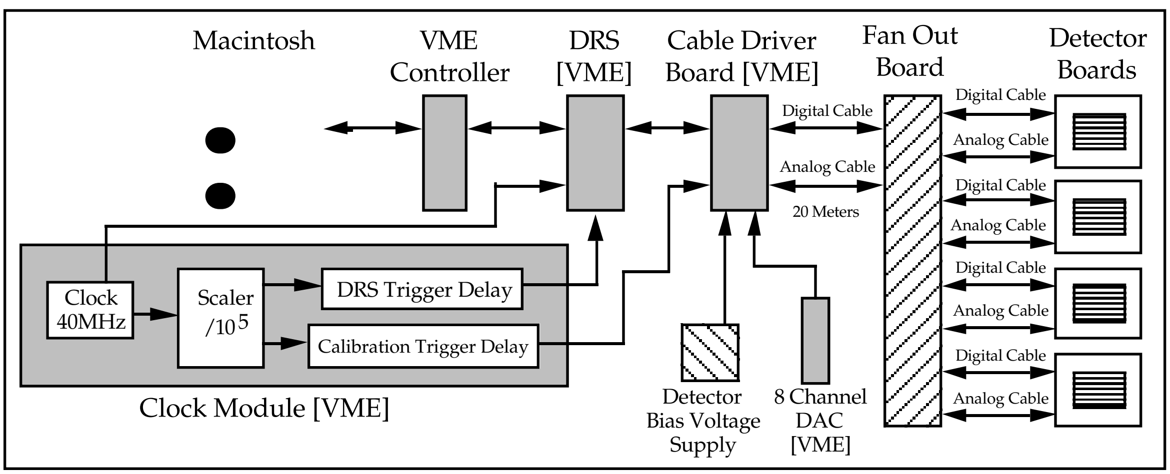

Figure 4 - Experimental set up.

---

6 Spencer et al. SCIPP 94/32.

7 The noise from the leakage current, in electrons, is; $N_i = \sqrt{\frac{2i\Delta t}{e}} \cdot F(\tau)$, $F(\tau)$ is some function of the shaping time of the amplifier and i is the leakage current.

The Macintosh talks to the VME crate[8] which houses the DRS [Digital Readout Sequencer], the Cable Driver Board, the Clock Module and the DAC [Digital to Analog Converter] through the VME Controller . The Macintosh also stores and analyzes the data collected.

The DRS reads the data collected from the read-out chips located on the detector board, and passes this data to the Macintosh.

The Cable Driver board mediates all the voltages and signals that are needed to run the read-out electronics on the detector board and sends them to the Fan Out board in two cables; analog and digital [for the analog and digital chips]. These cables are 20 meters long to meet specifications for the beam test at KEK.

The Clock Module provides the 40MHz clock signal which runs the entire system. It also provides the DRS trigger signal which synchronizes the delivery of data to the Macintosh. In addition, it supplies the Calibration Trigger signal which controls a calibration pulse, used for simulating particle signals in calibration and noise measurement..

The DAC is a power supply which supplies most of the voltages for the read-out electronics and can be set from the Macintosh.

The detector bias voltage is supplied by a HP Parameter Analyzer which also monitors the bias current.

The Fan Out Board takes the signals from the cable driver board and fans them out into four pairs of analog and digital cables which can be connected to up to four detector boards at one time.

The Detector and the Detector Board

A double sided, AC coupled, silicon microstrip detector manufactured by Hamamatsu was used for the experiment. It is 300 microns thick, 6cm long and 3.4cm wide. The strips have a pitch of 50 microns and a strip width of 10 microns [see figure 3]. The p-side strips are in stereo[9] [i.e. at an angle of 10mrad] to the n-side strips, which provides a two dimensional mapping of the particle position [figure 5].

---

[8] The VME crate is a box which holds various modules and provides them with basic power. It also, through the VME controller, mediates communication between the modules it houses and the Macintosh.

[9] Since the p-side strips are not parallel to the n-side strips they provide another spatial coordinate in order to determine the position of the particle penetrating the detector.

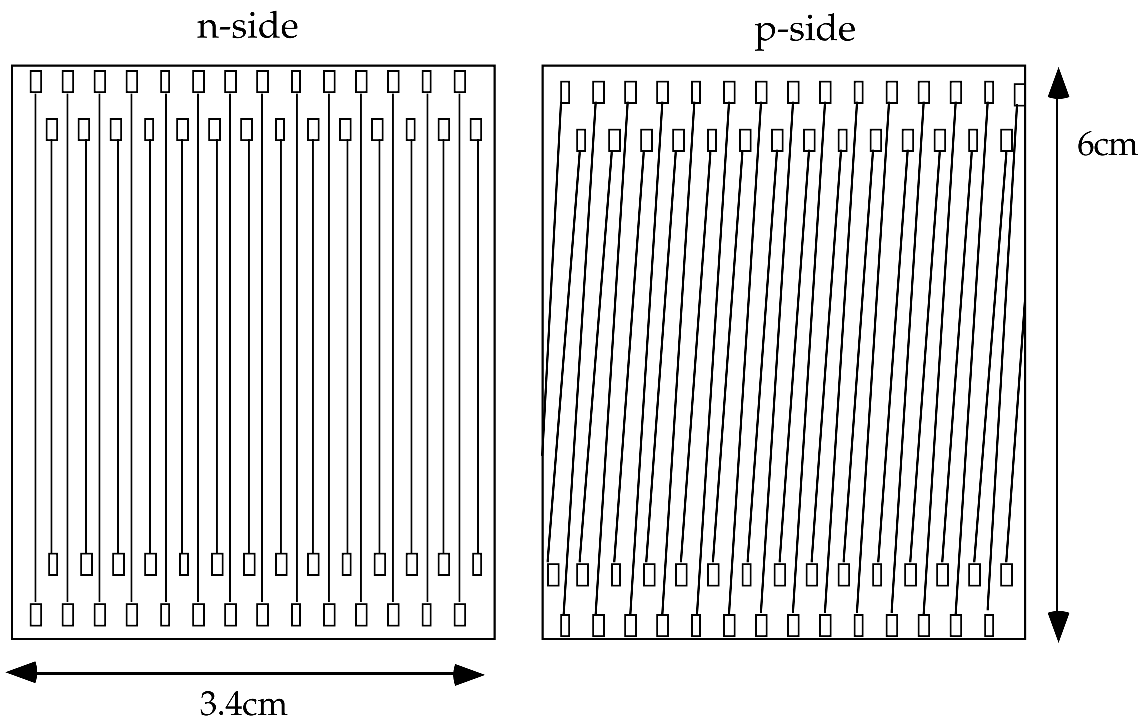

Figure 5 - The n and p-side of the detector [not to scale].

The detector is mounted on a hybrid detector board designed at SCIPP[10] [figure 6].

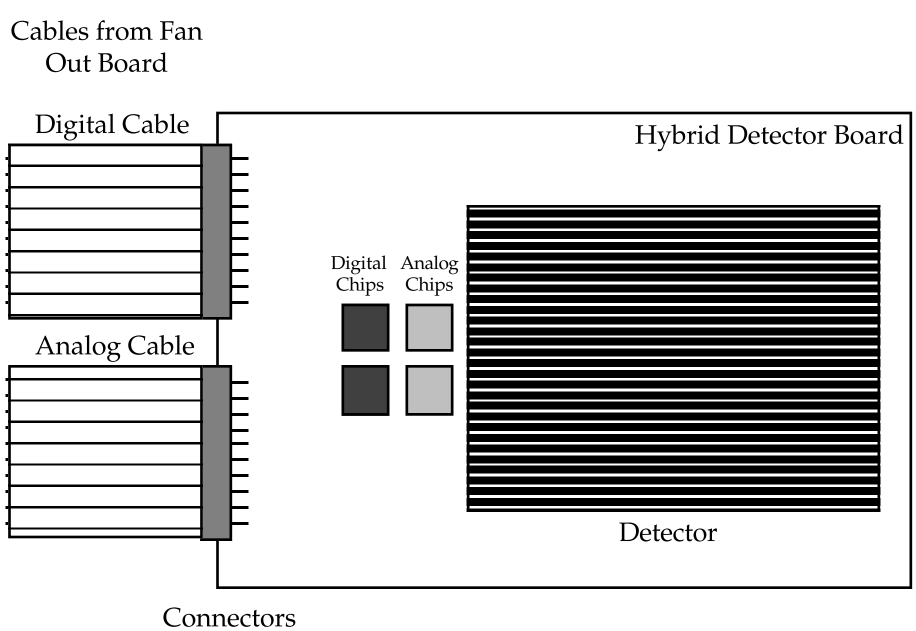

Figure 6 - Detector Board.

10 Santa Cruz Institute for Particle Physics

There are two pairs of readout chips on either side of the detector; an analog chip [the LBIC or Low Power Bi-Polar Integrator Comparator chip[11]] and a digital chip [the CDP or Clock Driven Pipeline chip[12]], which utilize 64 detector strips each[13].

The analog chip houses an amplifier and a comparator for each of the 64 channels. The amplifier takes a current input from a strip and produces a voltage signal which is presented to the comparator. The comparator has a threshold that can be varied [but is common to the chip] and it compares the voltage signal from the amplifier against this threshold. The output of the comparator is a logic signal; a 0 if the voltage signal from the amplifier is lower than the threshold, and a 1 if the signal is higher than the threshold voltage. An output of 1 is considered a hit. This logic signal is passed to the digital chip whose function is to store the signals. The digital chip has a storage bit for each strip and has a pipeline 80 bits deep [see figure 7].

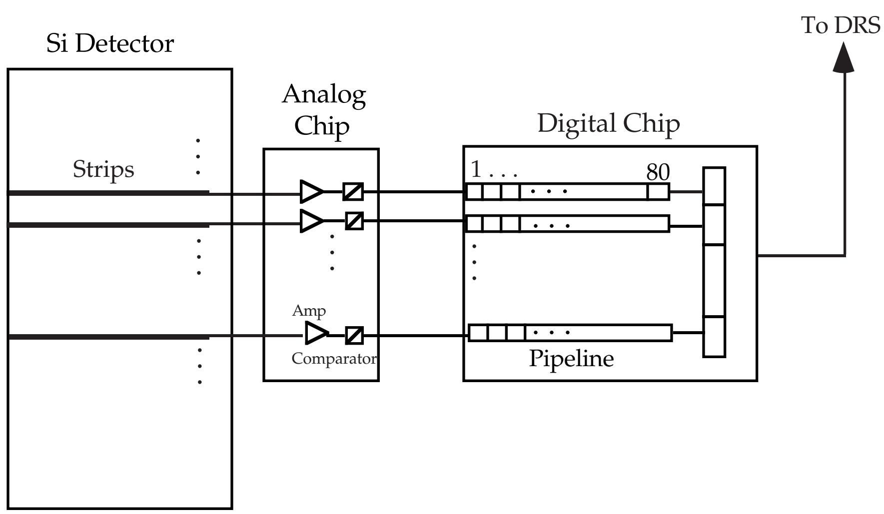

Figure 7 - Detail of detector and read-out electronics.

On every clock cycle the digital chip looks at the output of the comparator and stores a logic bit [a 0 or 1]. This signal, on the next clock pulse, moves over in the pipeline to make room for the next signal to be read in. A column of storage bits that are filled for all strips in one clock cycle are called a time slice.

---

11 Spencer et al. SCIPP 94/32.
12 DeWitt, SCIPP 93/37.
13 The chip has 64 channels where each channel can be connected to a detector strip.

These time slices can be read out of the digital chip by the DRS and passed to the Macintosh for final storage and analysis.

Noise Measurement Methods

Calibration Method

To measure the noise a calibration signal; a current signal presented directly to the input of the amplifier chip is used. In this way the noise from the detector is still collected, but a controlled, known signal is introduced so that the noise can be accurately measured. Actual signals caused by particles passing through the detector are not used to measure noise since their frequency and pulse height would not be known before they were detected.

The calibration signal is produced by four pulsers on the fan-out board. Each pulser provides a signal for sixteen channels, one fourth of the 64 channels for each chip. Therefore, we have four calibration lines; calibration lines 0, 1, 2 and 3. Calibration line 0 pulses channel 0, 4, 8, 12, 16 etc. where calibration line 1 pulses channel 1, 5, 9, 13, 17 etc.

The calibration pulse height is set using the DAC . Hardware response corrections are needed to obtain the correct input charge for a given voltage setting on the DAC. These corrections are detailed in the appendix.

It is important that the injected calibration signal is seen by the electronics. The digital chip looks at the output of the comparator on the rising edge of every clock cycle and therefore, there is some 'dead' time in which a signal could be present and not be recorded. A 'delay scan' [figure 8] is made where the delay between the calibration pulse and the clock pulse is varied and the occupancy [which is the percent of times that the signal was higher than the threshold] is recorded.

The delay curve for the p-side is much wider than for the n-side. This is because the voltage pulse from the amplifier on the p-side is much wider than for the n-side. The amplifier is designed to work with the p-side of a detector and therefore with positive signals. It is desirable for the output of the amplifier to be a long pulse so that the comparator does not miss it. The short pulse on the n-side however, is adequate, but not as reliable as the p-side.

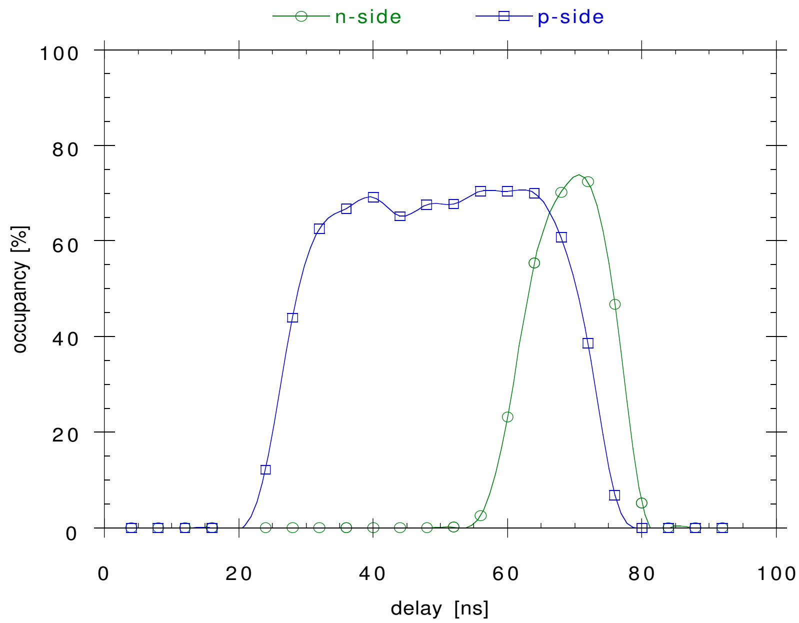

Figure 8 - Delay scan for n and p-side.

Since the threshold of the comparator can be varied, one can decide what size signals are registered as a hit. The size of the calibration signal can also be varied.

By varying the threshold while injecting a calibration signal of a fixed size, a 'threshold curve' is produced [figure 9].

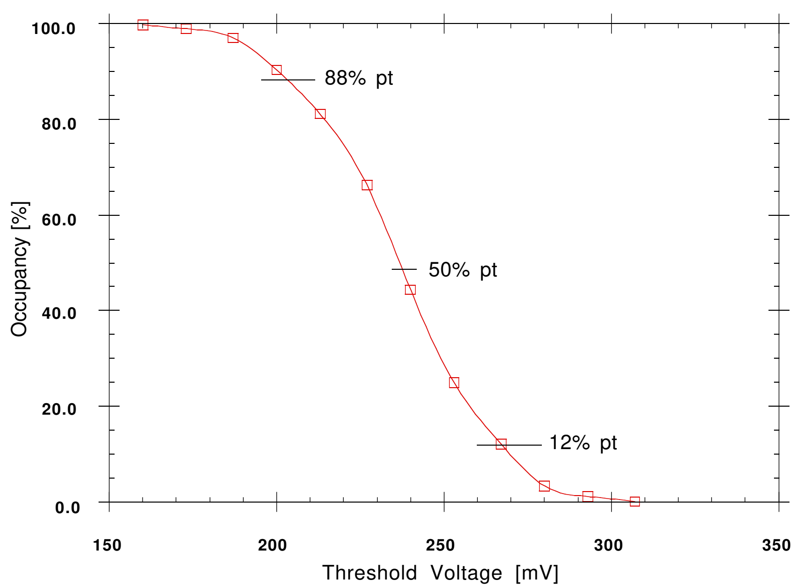

Figure 9 - Experimental Threshold Curve.

Ideally, if there were no noise, one would expect that a signal of constant size would always be registered as a hit until the threshold reached a level where it was just bigger than the signal [see figure 10A].

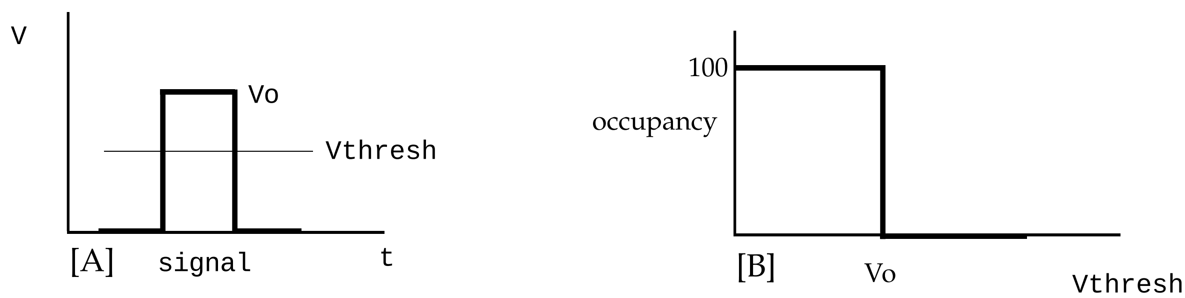

Figure 10 - [A] Simple square wave signal and [B] corresponding threshold curve.

If this were the case, the percent occupancy would sharply drop to zero as the threshold voltage became greater than the height of the signal [figure 10B]. But, as illustrated in the actual threshold curve [figure 9], there is rounding due to noise.

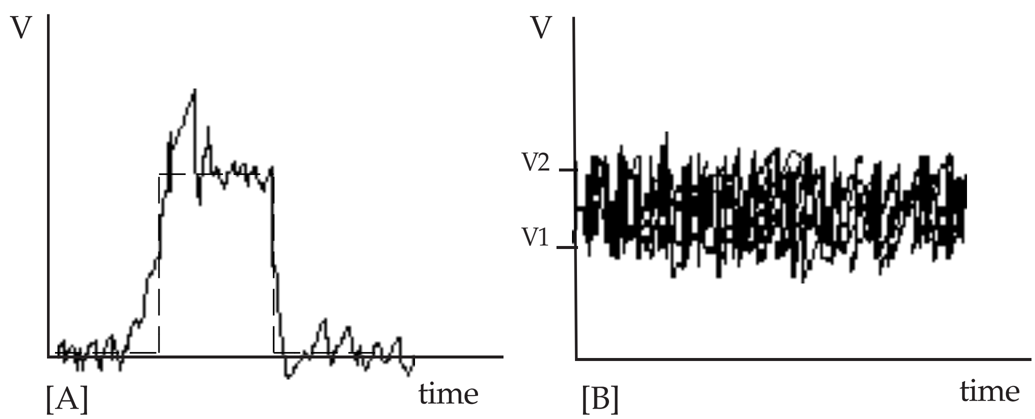

Figure 11 - [A] Signal with noise added. [B] Noise.

The noise distorts the shape of the signal, and can add or subtract to the signal [figure 11A]. Therefore, a hit may be registered when it should not have been [the noise has added to the signal height] or a hit may not be registered when one should have been [the noise has subtracted from the signal height]. If the noise is measured by itself a graph something like figure 11B obtained.

Since this noise causes the rounding of the threshold curve [i.e. we get figure 9 not figure 10B], the size of the spread due to the rounding, Γ, is equal to the amplitude of the noise: Γ = V2 - V1. Conventionally V1 is taken as the threshold voltage at the 88% occupancy point and V2 at the 12% occupancy point [these are marked in figure 9]. This gamma is the full-width-half-maximum [FWHM] of the noise distribution, which is 2.35 times sigma.

The noise distribution is the derivative of the threshold scan. A delta function, which is the signal without the noise, is the derivative of a theta function [or a step function, figure 10B]. The noise has a gaussian distribution. The derivative of an error function:

$$\mathrm{erf}(z) = \frac{2}{\sqrt{\pi}} \int_z^{\infty} e^{-z^2} dz, \quad z = \frac{|x-\mu|}{\sigma} \qquad [2]$$

is a gaussian:

$$P_G(x,\mu,\sigma) = \frac{1}{\sigma\sqrt{2\pi}} e^{-\frac{1}{2}\left(\frac{x-\mu}{\sigma}\right)^2} \qquad [3]$$

An actual threshold scan [figure 9] is the complementary error function:

$$\mathrm{erfc}(z) = 1 - \mathrm{erf}(z) \qquad [4]$$

Where sigma, σ, is the noise, μ is the median [which also is the 50% point of the threshold scan] and x is the threshold voltage. Sigma and mu are obtained by fitting the threshold scan to a complementary error function.

The measured sigma may be taken for the noise of the detector, but there are other things to consider. For example, the calibration signal is measured after going through the amplifier. The amplifier converts the current signal collected from the silicon strip, or injected at the input to the amplifier, into a voltage signal which can be compared against the threshold voltage. So the sigma, or noise, that we obtain from the threshold scan is the noise at the input to the comparator. We want to measure the noise at the input of the amplifier, i.e. the noise of the detector. In order to do this we must find out how the amplifier changes the signal, i.e. find the gain of the amplifier.

Gain, in general, is defined as the ratio of output over input. In this case we define the small signal gain [equation 5] as the difference in output voltage of the amplifier over the difference in input charge collected from the detector or injected at the input to the amplifier.

$$\text{Small Signal Gain} = \frac{\Delta \text{output voltage}}{\Delta \text{input charge}} \left(\frac{\text{mV}}{\text{fC}}\right) \qquad [5]$$

To obtain this number we take threshold scans for varying input charges [figure 12].

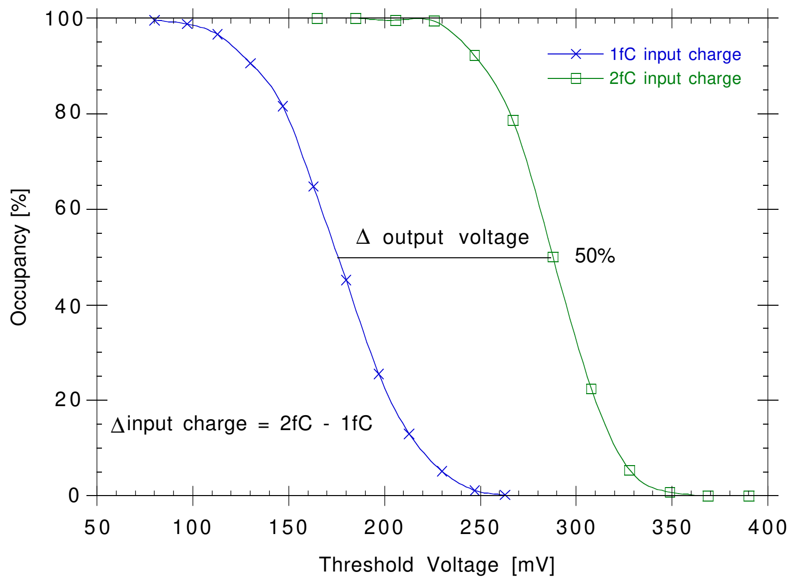

Figure 12 - Threshold scans for 1fC and 2fC input charges.

The difference in output voltage is taken as the difference in the 50% points of the two curves.

In practice, threshold scans are taken for five or more input charges and the 50% points are plotted versus the input charge [figure 13]. This is called the response curve. Taking the derivative of the response curve gives us the small signal gain.

As can be seen in figure 13, the response curve, for small input charges, is fairly linear but then begins to turn over. It can be fit to equation 6 which approximates its observed behavior. It is linear for small Q and saturates for large Q.

$$V = A + B\left[1+\left(\frac{B}{C\cdot Q}\right)^{2}\right]^{-\frac{1}{2}} \qquad [6]$$

Where A, B and C are parameters. Table I lists experimental values for these parameters for different strip length.

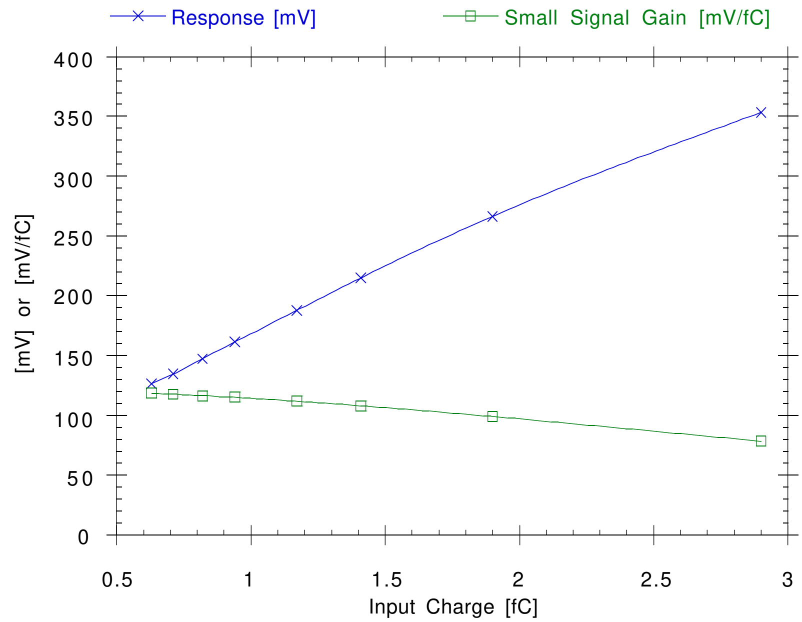

Figure 13 - Sample response and small signal gain curve.

Table I - Parameters from the fit of the response curve.

strip length [cm]		A	B	C
0	n-side	47	560	132
	p-side	43	600	150
6	n-side	45	560	143
	p-side	44	578	157
12	n-side	57	488	122
	p-side	68	658	142

The slope of this curve at any point is the small signal gain at that point.

$$\frac{dV}{dQ} = \frac{B^3}{C^2 Q^3}\left[1+\left(\frac{B}{C \cdot Q}\right)^2\right]^{-\frac{3}{2}} \qquad [7]$$

Values for A, B and C from the fit of the response curve are used to calculate the small signal gain for different input charges.

Now the noise at the input to the amplifier can be computed. The noise is the ratio of sigma and small signal gain;

$$\text{noise} = \frac{\sigma}{\text{sm. signal gain}}. \qquad [8]$$

The response, the small signal gain, the sigma and the noise curves as a function of input charge are presented together in figure 14.

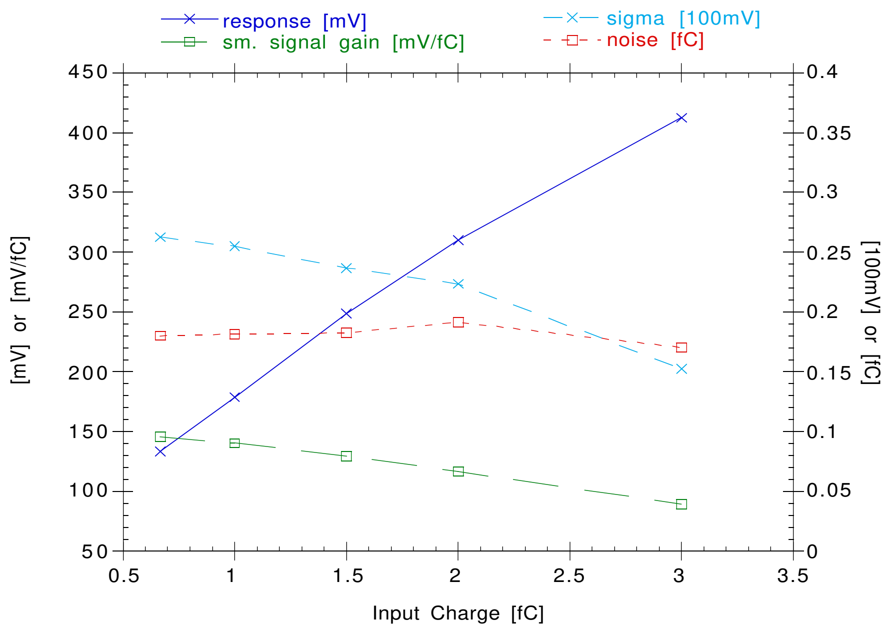

Figure 14 - Sample Graph of Results.

The noise measured should be independent of the input charge used. This is true in figure 14 for small input charges, but the 3fC point is lower than the others. This is due to the fact that the response curve is not fit well for large input charges. The rounding of the response curve at high input charges is not well understood. Whereas, the small differences in the noise for lower input charge is mostly statistical.

<u>Considerations</u>

Number of Counts/Threshold. We found that in taking a threshold scan, the number of counts per threshold used greatly affected the noise measurement. This is mostly due to the statistical error for different counts. We took threshold scans with 200 counts/threshold and then 500 counts/threshold which have statistical errors of 7% and 4.5% respectively. Figure 15 is a plot of the noise vs. input charge for the different situations.

The effect is from the fit of the threshold scan to a complementary error function. Since there is a larger error on the occupancy points for 200 counts/threshold the fit is worse than for 500 counts/threshold. This can be seen by comparing the sigma's which are computed from the fit of the threshold scan [figure 16].

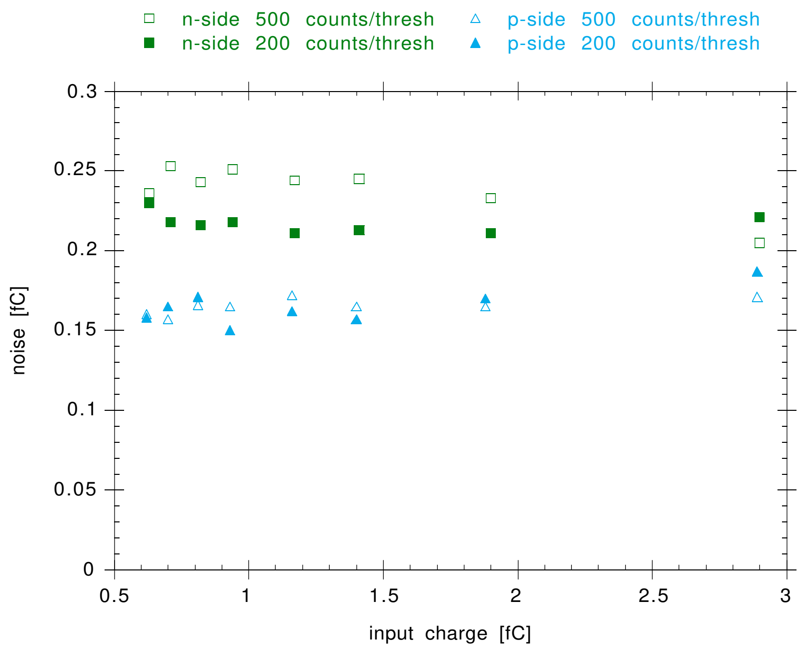

Figure 15 - Noise Comparison for 200 vs. 500 counts/threshold [6cm strips].

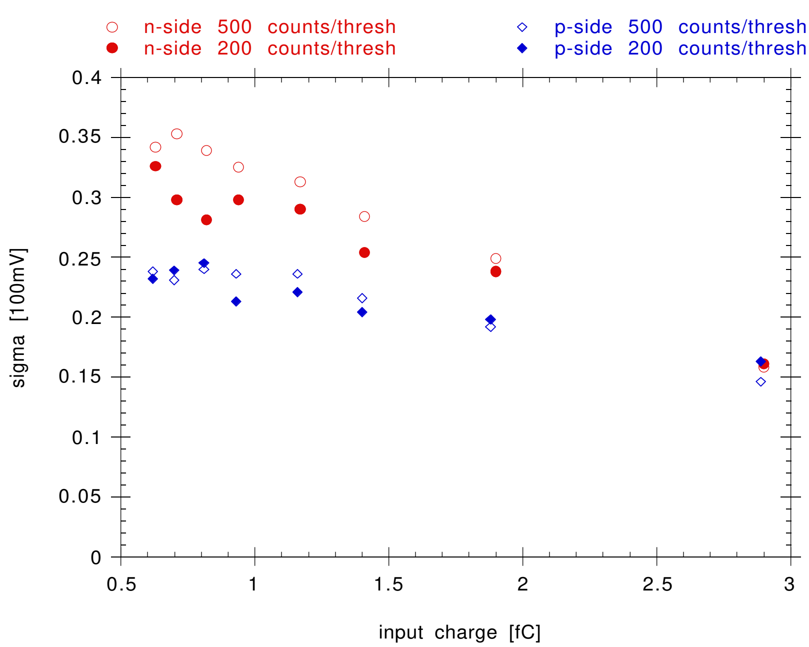

Figure 16 - Sigma Comparison for 200 vs. 500 counts/threshold [6cm strips].

The trend of the data is the same for the noise and the sigma. Since noise is sigma divided by small signal gain and the noise and sigma exhibit the same behavior, we can infer that the small signal gain for 500 and 200 counts/threshold is the same. We then know that the response is also similar for both cases since the small signal gain is the derivative of the response. The response and the sigma both are obtained from the fit of the threshold scan, but the sigma is more sensitive to errors in the occupancy.

Different Number of Input Charges. To examine how sensitive the fit of the response curve is, the difference in noise depending on the number of input charges used in analysis of the data is examined. The number of input charges used give the number of points that define the response curve. If the fit of the response curve changes the values for the small signal gain will also change.

Data was usually taken for eight different input charges; approximately 2/3, 3/4, 7/8, 1, 1.25, 1.5, 2 and 3 fC. In figure 17 the noise obtained for analysis of the same data run with all eight input charges and with only four; 2/3, 1, 1.5 and 2 fC is shown to match. Therefore we can conclude that the fit of the response curve did not change significantly.

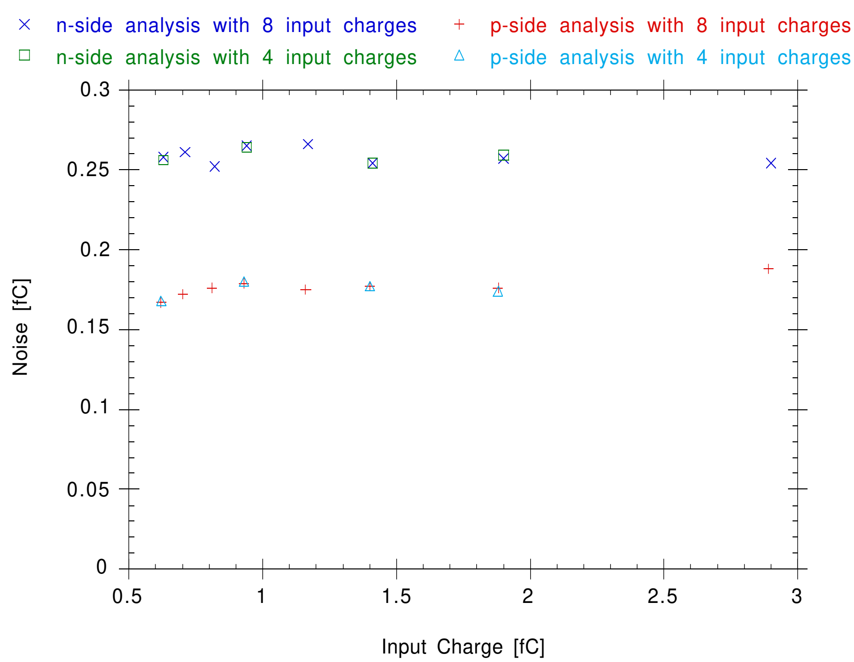

Figure 17 - Noise Comparison for Analysis with 8 and 4 input charges [6cm strips].

Consistency Over Time. To check consistency data was collected with the same conditions two days apart [Figure 18]. The results for the different days are consistent to within 5%, implying that our measurements are only valid to 5%.

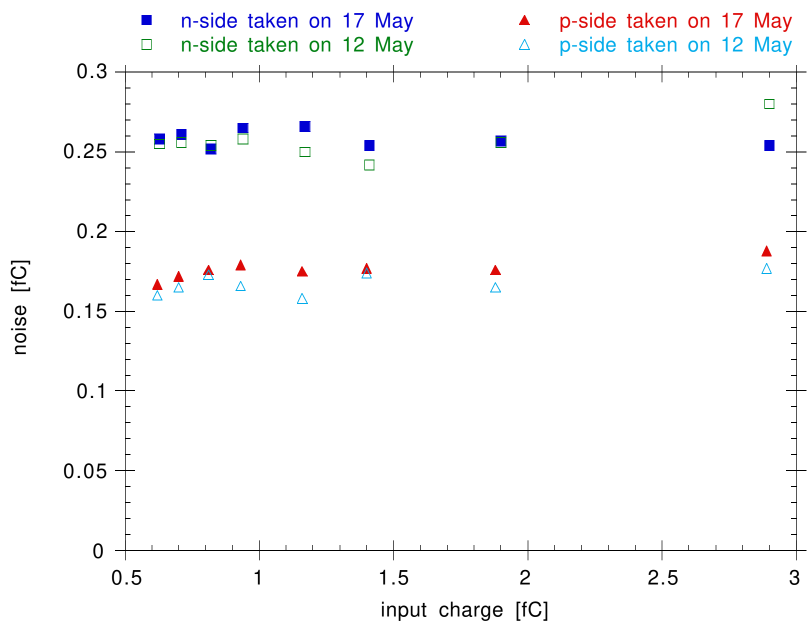

Figure 18 - Comparison of Noise Measurements done on two different days [6cm strips].

Grounded Neighbors. We attempted to isolate a single strip by connecting its nearest neighbors to ground. In this way the noise contribution of the neighboring amplifiers can be eliminated.

The nearest neighbors were connected at the end of the detector to a large grounded plane on the detector board and noise measurements were taken. In analyzing the data it was found that the signal had been greatly distorted by pick up of the clock signal. The ground plane acts like an antenna, picking up and adding the high frequency clock signal to the pulse we were trying to measure. This can be seen by looking at a delay scan for this configuration [figure 19].

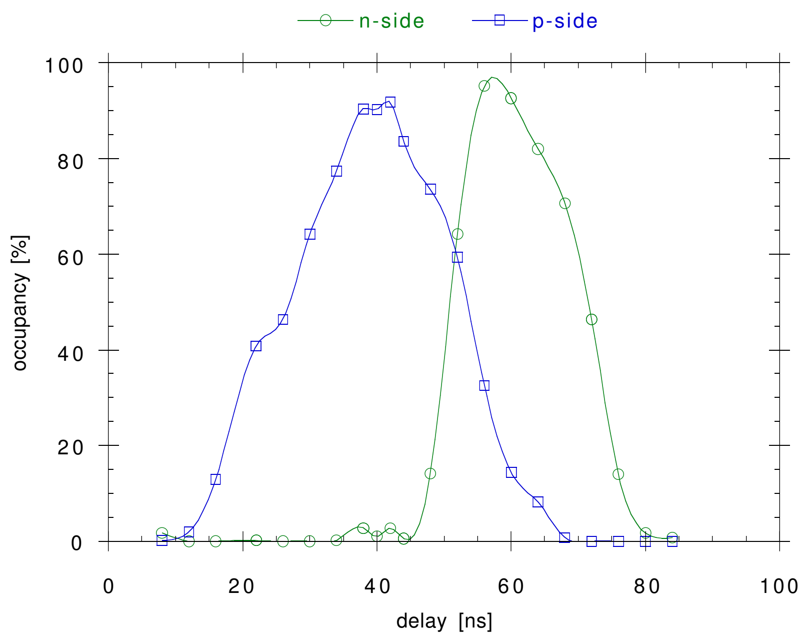

Figure 19 - Delay scan for a 6cm strip with nearest neighbors to ground.

The nice flat behavior of the delay scan for the p-side [figure 8] has been destroyed by the clock pick up. This can be avoided by connecting the strips to the same ground the comparator in the analog chip uses as a reference. Therefore any ground fluctuations will be the same for the signal being measured and for the threshold voltage of the comparator, leaving the measurements unaffected.

Occupancy Method

For the occupancy method of measuring the noise no signal, real or injected is used. The noise becomes the signal measured. As stated before, the noise has a gaussian distribution and therefore, the threshold scan is described by a complementary error function [see equations 2 and 3]. Occupancy is measured as the threshold is raised from a value close to zero, We can use a gaussian approximation or a numerical solution to the complementary error function to fit the data.

Gaussian Approximation

The noise distribution as a function of threshold voltage can be approximated by a gaussian[14];

$$N = N_o e^{-\frac{1}{2}\left[\frac{V_T}{\sigma}\right]^2}, \qquad [9]$$

where N is the occupancy at a certain threshold, N_o is the occupancy at a threshold of 0 Volts, V_t is the threshold voltage in mV, and σ is the noise in mV. We would like the noise in fC so that we can compare with the noise measured using the calibration method. V_t can be converted into an equivalent input charge. Looking at the response curve [figure 13] the input charge for any given threshold in mV can be read off. The gaussian equation then becomes;

$$N = N_o e^{-\frac{1}{2}\left[\frac{Q_{in}}{\sigma}\right]^2} \qquad [10]$$

where Q_{in} is the equivalent input charge and σ is now the noise in fC.

The occupancy for various thresholds is measured. The noise is a fairly small signal and so we must take a large number of counts in order to obtain enough statistics. This gives us the values for N and V_t.

Taking the natural log of both sides of the gaussian gives:

$$\ln[N] = -\frac{1}{2\sigma^2} Q_{in}^2 + \ln[N_o] \qquad [11]$$

Plotting ln[N] vs. Q_{in}^2 a straight line is obtained [figure 20], where the $\text{slope} = -\frac{1}{2\sigma^2}$ and the y intercept = $\ln(N_o)$.

With the value for the slope obtained from a linear fit of the data one can solve for sigma to obtain a value for the noise in fC:

$$\sigma = \sqrt{1 \big/ -2 \cdot \text{slope}} \qquad [12]$$

The occupancy for zero input charge, N_o [$N(0) = N_o$] can also be computed.

One can see that figure 20 is not really a straight line. This is because the equation used to fit the data is only an approximation. Therefore, the value for the noise that is obtained from a straight line fit to all the data is not very accurate. We can claim that the approximation breaks down for small input charges, and use only the fairly linear points in figure 20 [the points from Q_{in}^2 =

14 Rice, p. 282.

$0.1 fC^2$ up] to do the linear fit. In this way a more accurate value for the noise is obtained.

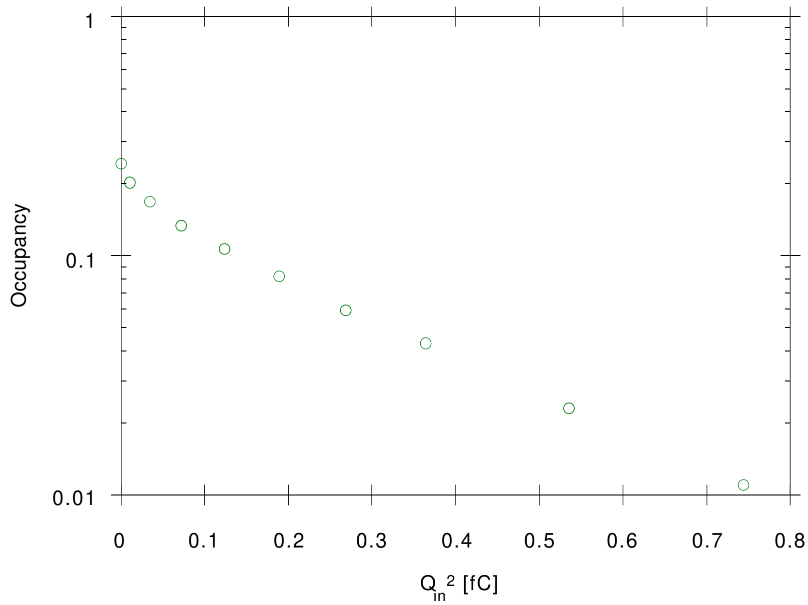

Figure 20 - Graph of ln[N] vs. Q_{in}^2.

To obtain an accurate result for this method the behavior of the data close to zero must be ignored. Therefore the N_o that is measured does not correspond to the true occupancy at zero threshold voltage and does not hold any physical significance.

<u>Complementary Error Function</u>

Figure 21 shows a plot of the complementary error function and a gaussian. Comparing these with the data [figure 20] we see that the complementary error function has the same behavior as our data for small input charge.

A numerical solution to the complementary error function [equation 4] can be used to fit the data. Now instead of equation 10 we have;

$$N = N_0' \operatorname{erfc}(z) \qquad [13]$$

Data is taken as above, and the response curve is used to convert the threshold voltage into an equivalent input charge. Fitting this to a complementary error function, a value for sigma [the noise] and for the occupancy at zero threshold voltage is obtained.

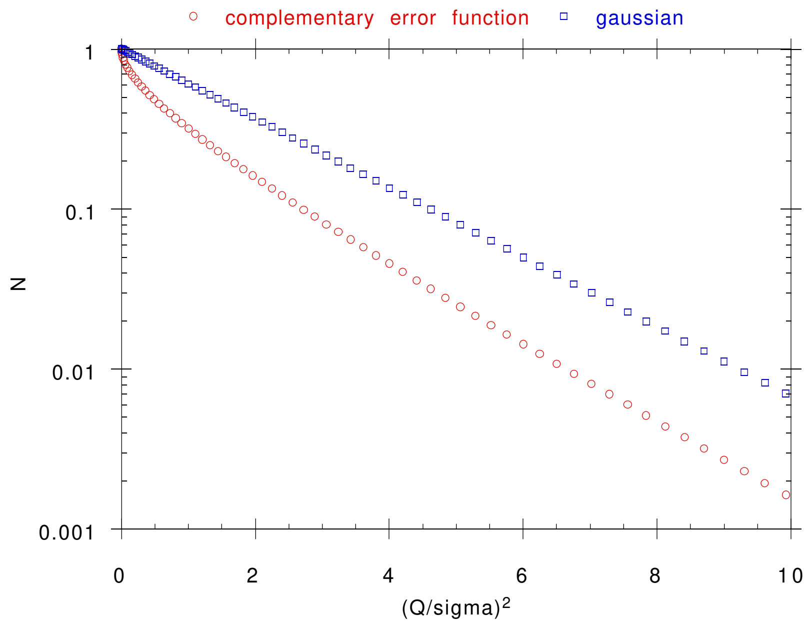

Figure 21 - Plot of complementary error function and gaussian.

Since we are now taking into account the data for both small and large input charge, N'_o is the true occupancy for zero threshold voltage. N'_o is a measure of the frequency of noise[15]. When the threshold voltage is at zero volts all positive noise fluctuations are collected. N'_o depends on the bandwidth of the amplifier[16] and the frequency of the clock signal that controls the readout electronics.

For the occupancy method we rely heavily on the response curve generated by the calibration method to convert the threshold voltage into an equivalent input charge. With the occupancy method we are measuring noise fluctuations which have equivalent input charges that are almost all less than 1fC. But, in the calibration method the lowest input charge that we inject is 2/3 fC. Therefore, for the occupancy method, a range on the response curve is used which is not experimentally known. The behavior for low input charge is extrapolated from the equation with which the response curve is fit. The assumption that this equation is also valid for small input charge may not be correct.

15 Spieler, p. 5.
16 The bandwidth is the frequency range that the amplifier will pass.

IV. RESULTS AND DISCUSSION

All of the following noise measurements were made using the calibration method unless otherwise noted. The measurements are from the same detector, read-out chips, and strips. Only one calibration line was measured in order to minimize systematic errors and the time for data collection. All measurements were taken with the detector fully depleted at a bias voltage of 80 Volts. For the calibration method, all noise figures are quoted at 1fC input charge and averaged over all channels with the same strip length, unless otherwise noted.

Materials on Top of the Detector

A new development in hardware for silicon strip detectors is a detector board made out of Kapton [a type of plastic] instead of G-10 [a fiberglass material which is used to make circuit boards]. This Kapton hybrid is much smaller than the current detector board and can be mounted directly on top of the detector. However, having material on top of the detector could possibly change the capacitance between strips and therefore the noise. To investigate this possibility various materials were placed directly on top of the detector [figure 22] and the noise was measured [table II]. The materials used were G-10 , alumina [aluminum oxide] and aluminum. Measurements were taken for both 6cm and 12cm strips.

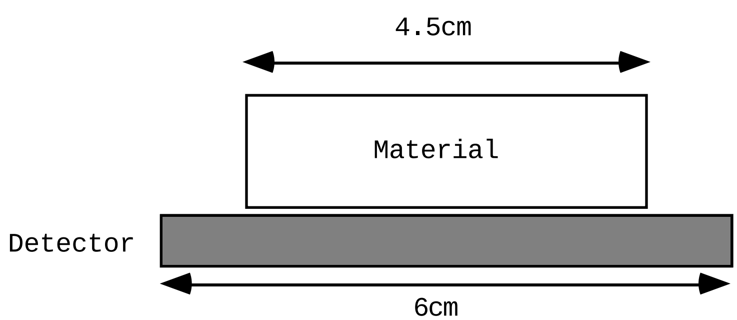

Figure 22 - Material placed directly on top of the detector.

Table II - Noise results for 6cm and 12cm strips with various materials.

		noise [fC]
6cm strips	p-side	0.175
6cm w/ G-10 (354μm thick, 2in long)	p-side	0.179
6cm w/ Alumina (630μm thick, 2in long)	p-side	0.183
6cm w/ Aluminum (373μm thick, 2in long)	p-side	0.181
12cm strips	p-side	0.283
12cm w/Aluminum (630μm thick, 4in long)	p-side	0.304
12cm strips	n-side	0.440
12cm w/Aluminum (630μm thick, 4in long)	n-side	0.452

The differences in noise when these materials were placed on the detector were from 2 to 7 percent, and we know that we already have a 5 percent error on our measurements. Therefore, we can conclude that the noise did not change when materials were placed on the detector.

The fact that the noise did not change was a surprising result. It was expected that by placing material directly on top of the detector the capacitance from each strip to its nearest neighbors would change and therefore the noise would change. But, even when aluminum was placed on top, which would have the most drastic effect since it is a conductor, there was no change in the noise.

To try to explain the invariance of the noise in this situation, one can calculate of what one would expect the change in capacitance, to be with a conductor placed on top of the detector. The conductor is not sitting flat or touching the detector; there is air in between. The situation looks approximately like that drawn in figure 23.

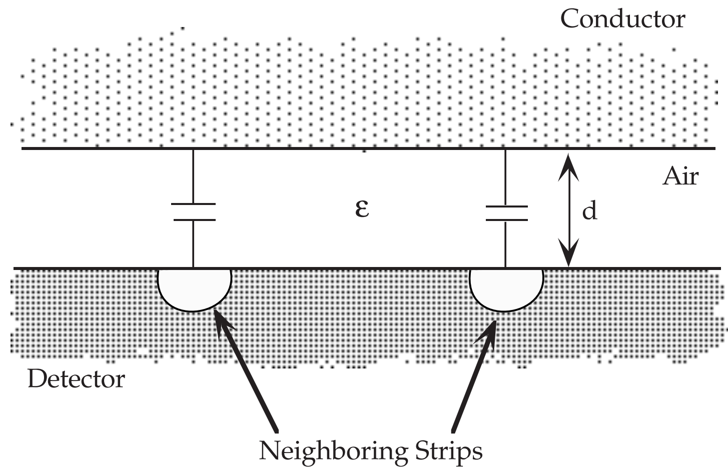

Figure 23 - Added capacitance by placing material on top of detector.

We can calculate the added capacitance, ΔC ;

$$\text{since} \quad C = \frac{\varepsilon A}{d} \quad \text{our} \quad \Delta C = \frac{\varepsilon A}{2d} \qquad [14]$$

Where ε is the permittivity of air, A is the width of the implant strips times the length of the material and d is the distance between the conductor and the detector.

Our hypothesis for why an effect from the increased capacitance was not seen is that the material was too far away from the detector to have a noticeable effect. We can assume that if the effect is less than 10% it can not be detected. We can then calculate the minimum d for a 10% change in C per length. The minimum d turns out to be approximately d = 10μm. This is very close, and for the above measurements the material was probably more in the range of 100μm away from the detector. This explains why an effect was not seen. A simulation was also done which confirmed this hypothesis[17].

To examine this effect, a way to make the material either closer to the detector or couple it to the strips was needed. To do this a drop of distilled water was placed on top of the detector and then a sheet of Kapton [56μm thick, 4.5 cm long] was placed on top of the water drop and used to spread out the water. In this way a thin film of water covered by Kapton was made.

Taking noise measurements, with the Kapton and water on top of the p-side of the detector it was found that the noise did increase [table III].

[17] Johnson [1995]

Table III - Noise for 6 and 12cm strips with and with out Kapton and water film

	noise [fC]
6cm strip	0.175
6cm with water film and Kapton	0.246
12 cm strip	0.304
12 cm with water film and Kapton	0.392

This increase in noise is from both the effect of the water film, since ε of water is quite large, and the Kapton.

6cm Strip Configuration

Noise measurements were made for 6cm strips [figure 24 and table IV]. These strips are all connected to their amplifier as were all of their neighbors.

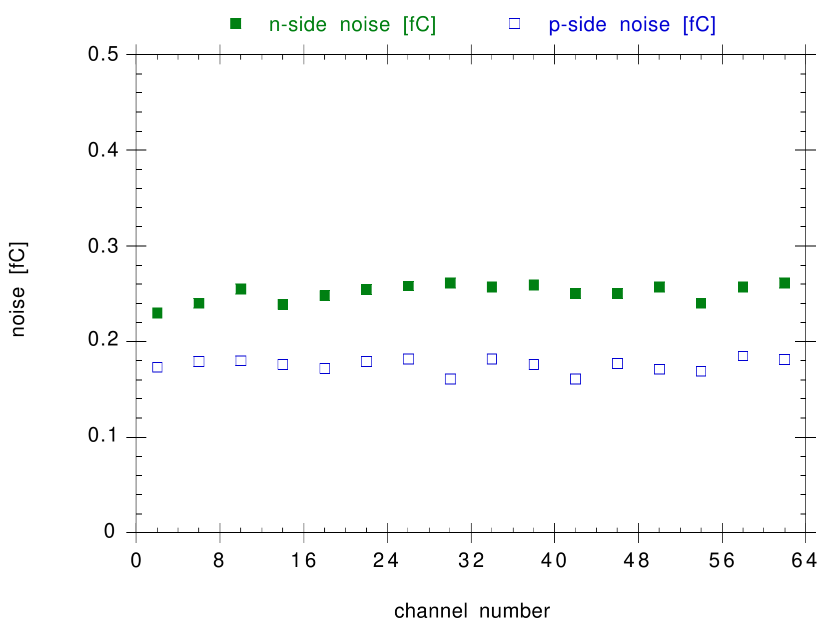

Figure 24 - Noise for 6cm strip configuration.

Table IV - Noise for the 6cm strips.

	noise [fC]
n-side	0.251
p-side	0.175

The noise across the channels is fairly uniform with a standard deviation of about 4%.

The noise for the n-side of the detector is larger than for the p-side. This is because the n-side has a higher capacitance than the p-side for a bias voltage of 80V[18]. The capacitance depends on the size of the depletion region, which depends on the bias voltage. At a bias voltage of 80V the detector has just become fully depleted. If the bias voltage is increased the capacitance for the n and the p-side level out and become equal. We chose to run the detector at 80V because applying a much higher voltage to the detector could damage it by breaking down the coupling capacitors between the implants and the metal strips.

12cm Strip with Four Neighboring Amplifiers Configuration

Two strips were wire bonded[19] together effectively making a 12cm-long strip. Seven strips still connected to their amplifiers were left in between each pair. The strips were connected at the far end of the detector, away from the electronics, and one of the pair was disconnected from its amplifier [figure 25].

---

18 Nibarger, Thesis.

19 Wire bonding is a method of connecting strips together with thin [1mil diameter] gold or aluminum wire. The wires are ultrasonically fused to the strips which have gold pads at both ends of the detector designed specifically for this. The strips are also connected to the electronic chips in this way. The wire bonding done for the measurements presented in this paper were highly unusual and difficult.

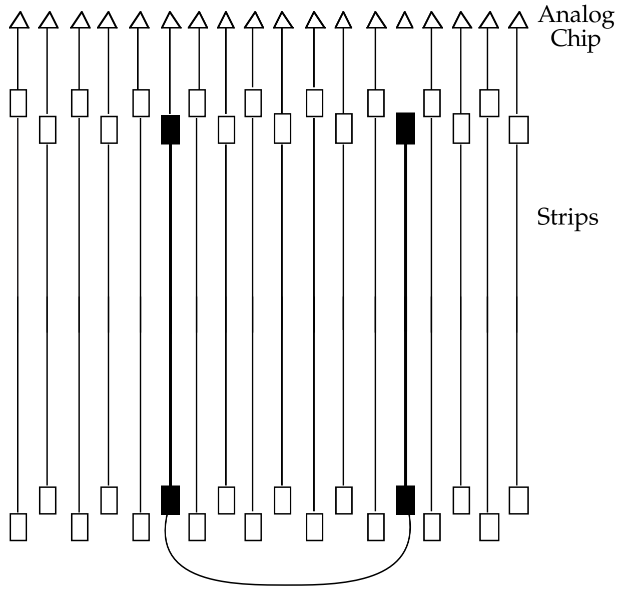

Figure 25 - 12cm with 4 neighboring amplifiers configuration. Two 6cm strips bonded together [highlighted ones] to form a 12 cm strip.

The noise was then measured for this configuration. The results are presented in figure 26 and table V. The noise for the 12cm strips is higher than for 6cm strips, which is expected due to the increase in resistance and capacitance for a longer strip. In this configuration there is a noise contribution from four neighboring amplifiers since the 12cm strips have four 6cm neighbors. The noise for this configuration will be higher than if we had a detector with 12cm strips, where the 12cm strip would have two 12cm neighbors, but by how much still has to be determined.

In figure 26 the noise is presented for 0, 6, and 12cm strips. A 0cm strip is a channel that has been disconnected from the detector, therefore only the noise from the electronics is measured.

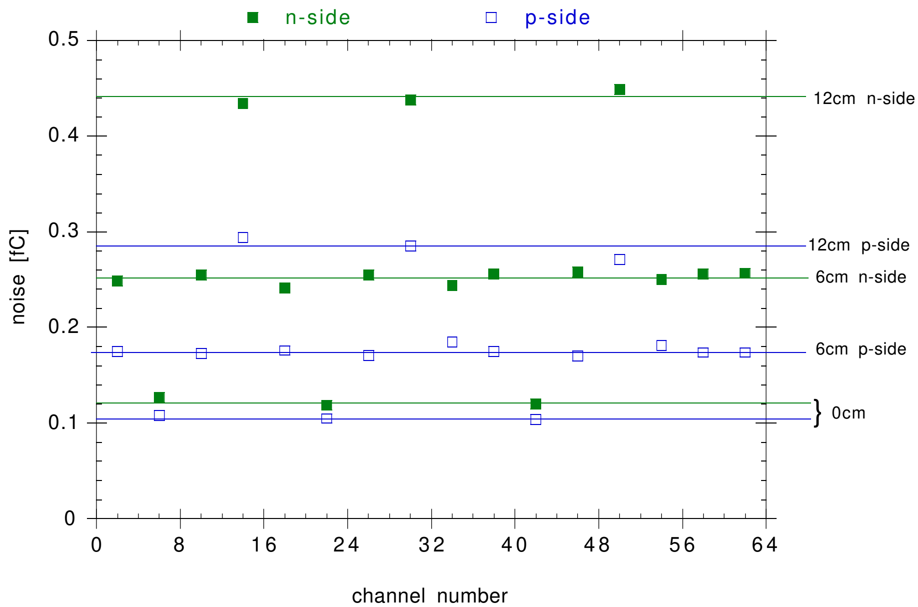

Figure 26 - Noise for 12cm with 4 neighboring amplifiers configuration

Table V - Noise for 12cm strips with 4 neighboring amplifiers.

	noise [fC]
n-side	0.440
p-side	0.283

12cm Strip - Middle Configuration

Two 6cm strips were connected together near the electronics forming 12cm strips with the read-out electronics in the middle [figure 27]. In order to do this it was necessary to remove the bonds to the analog chip on the strips in between the two test strips. These interior strips were left floating. The nearest neighbors to the test strips were also connected together at the end of the detector, forming effective 12cm neighbors. With 12cm neighbors there is a noise contribution from only two neighboring amplifiers which would be the case if we had an actual 12cm long detector. There only is a noise contribution from an amplifier when it is bonded to a strip.

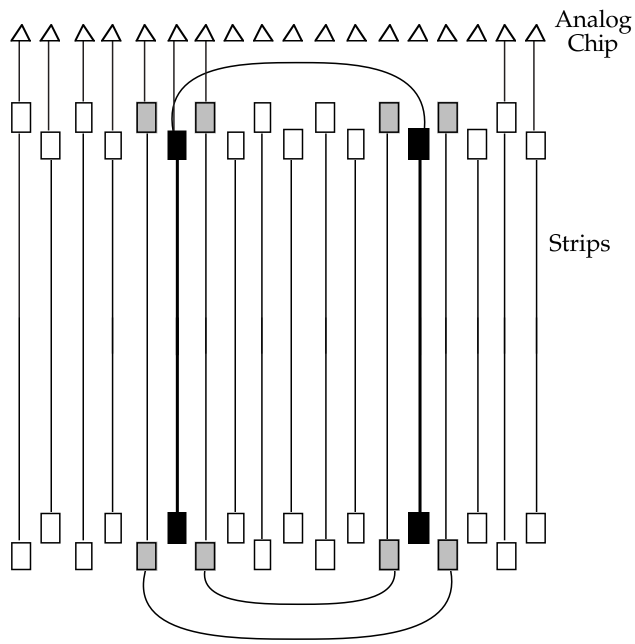

Figure 27 - 12cm - middle configuration. Two 6cm strips bonded together near the electronics [shaded black] to form a 12 cm strip with 12cm nearest neighbors [shaded gray].

We measured the noise for this configuration [figure 28 and table VI].

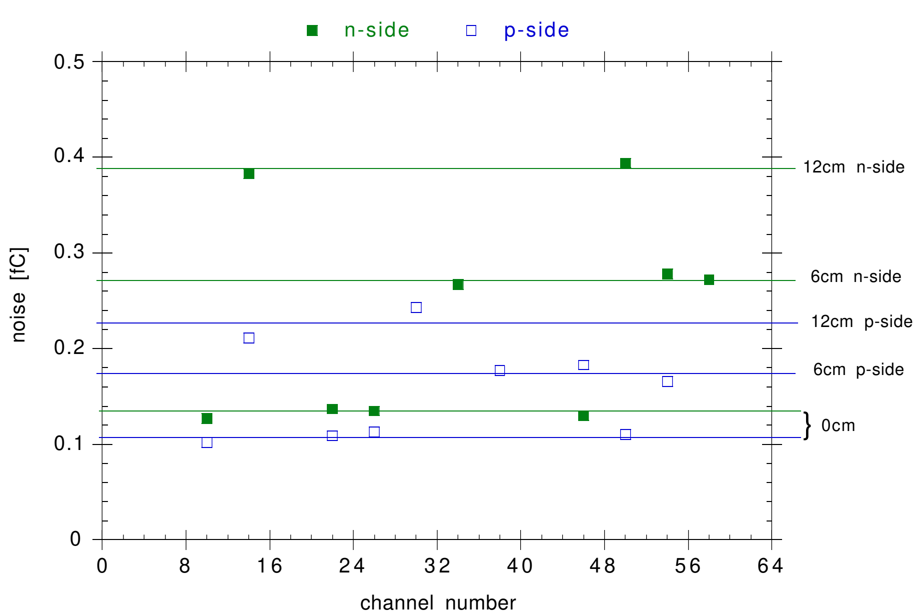

Figure 28 - Noise for 12cm - middle configuration.

Table VI - Noise for 12cm strips connected at the middle.

	noise [fC]
n-side	0.389
p-side	0.227

This configuration eliminates the contribution of two extra amplifiers but creates floating strips in between and around our test strips. Floating strips pose a problems since we do not know how to determine the capacitance they have. The nearest neighbor to a strip gives the largest noise contribution. The floating strips are at least one strip away from our test strips [the 12cm ones], and so their unknown contribution to the noise should not be a large effect, but we have not tested this hypothesis.

12cm Strip - End Configuration

The pair which was connected in the middle was disconnected and reconnected at the end instead. The strips in-between were left floating and the neighbors connected to form 12cm strips [figure 29].

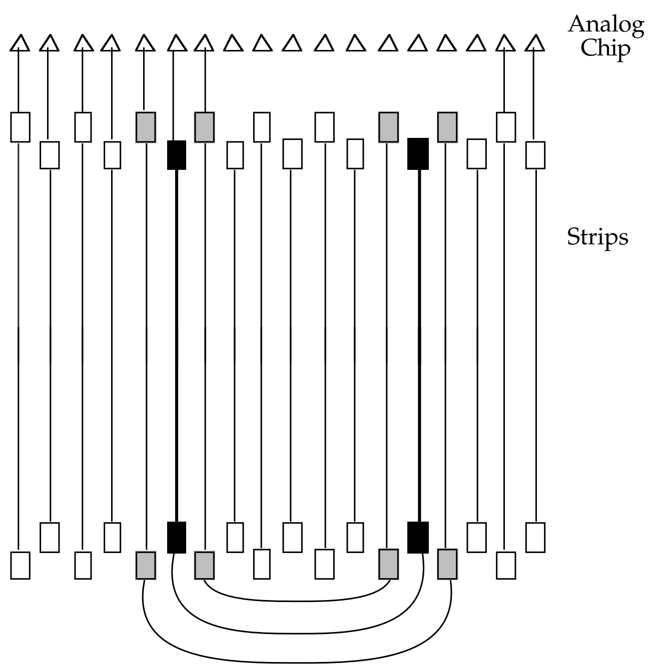

Figure 29 - 12cm - end configuration. Two 6cm strips bonded together at the end of the detector [shaded black] to form a 12 cm strip with 12cm nearest neighbors [shaded gray].

The noise for this configuration was measured [figure 30 and table VII].

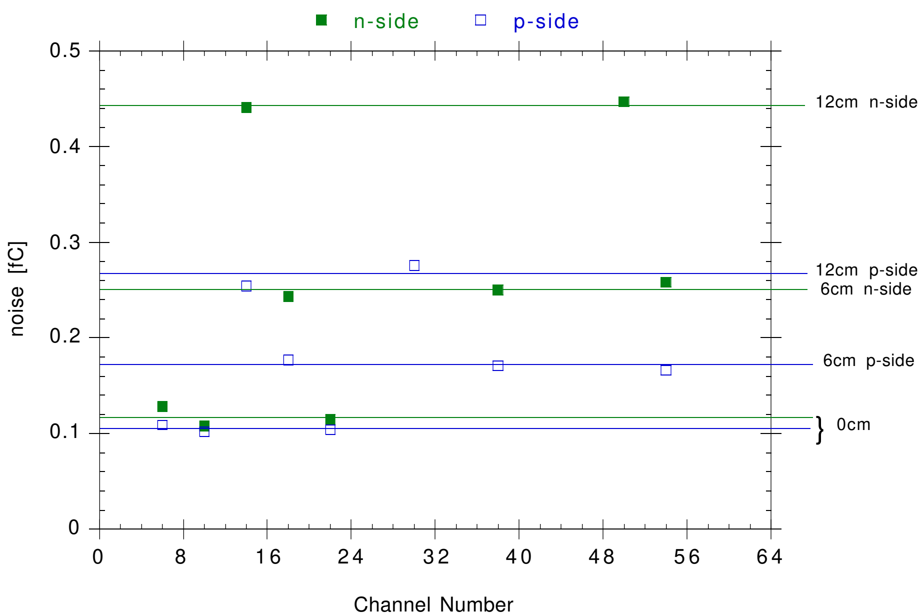

Figure 30 - Noise for 12cm - end configuration.

Table VII - Noise for 12cm strips connected at the end.

	noise [fC]
n-side	0.444
p-side	0.265

This configuration is also complicated by the unknown capacitance of floating strips.

Occupancy Method

We used the occupancy method to determine the noise for the 12cm - end configuration.

Gaussian Approximation

Figure 31 and table VIII illustrate the results that were obtained using a gaussian approximation to analyze the data.

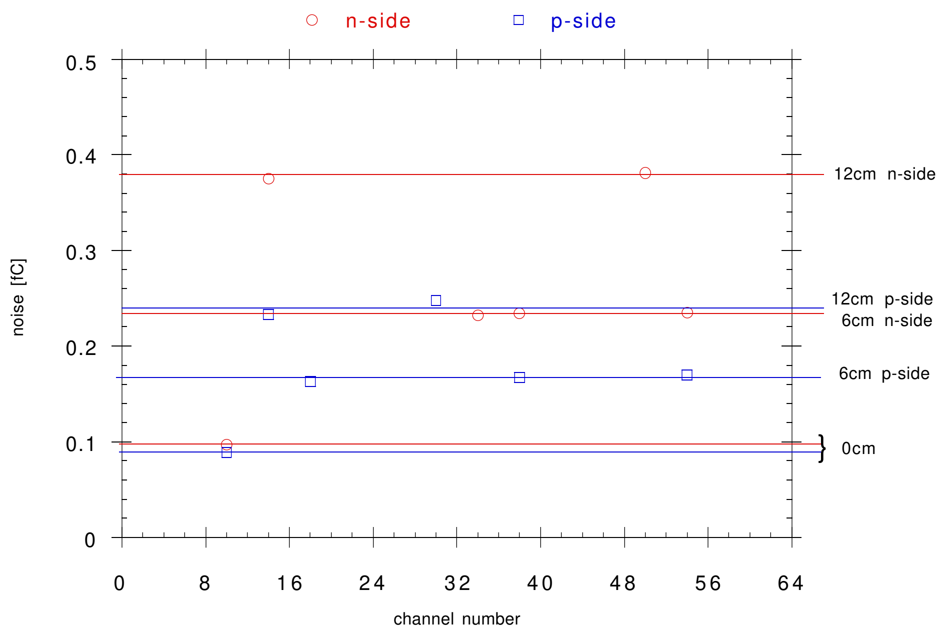

Figure 31 - Noise obtained for the occupancy method using the gaussian approximation.

Table VIII - Noise for 0, 6 and 12cm - end strips for the occupancy method using the gaussian approximation.

	noise [fC]	
	n-side	p-side
0cm strip	0.097	0.089
6cm strip	0.233	0.167
12 cm strip - end	0.378	0.241

Complementary Error Function

A numerical solution to the complementary error function was used to fit the data. The results are presented in figure 32 and table IX.

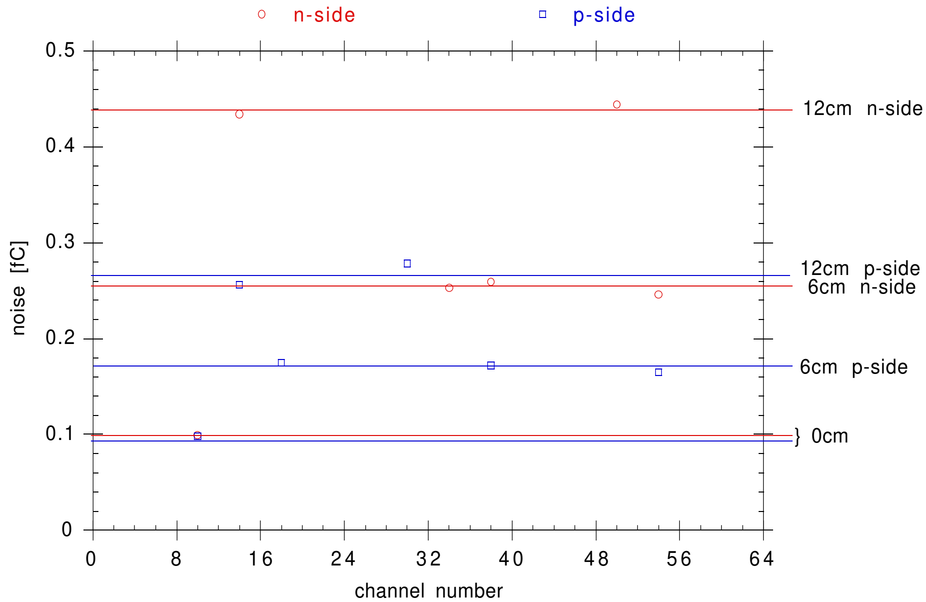

Figure 32 - Noise obtained for the occupancy method using the complementary error function

Table IX - Noise for 0, 6 and 12cm - end strips for the occupancy method using the complementary error function.

	n-side		p-side	
	noise [fC]	N'_o	noise [fC]	N'_o
0cm strip	0.099	0.24	0.098	0.38
6cm strip	0.253	0.44	0.171	0.82
12 cm strip - end	0.439	0.50	0.267	0.78

For the p-side of the detector, the output of the amplifier is a longer pulse than for the n-side and so there is a greater chance that an incoming pulse will be recorded in the digital chip. Therefore, the value for N'_o for the p-side is larger than for the n-side.

The N'_o's for the 6 and 12cm strips are fairly similar, while the values for the 0cm strips are significantly lower. The 0cm strips have low noise and so all of the data points are in the low input charge range where the behavior of the response curve is not known. Therefore, the noise and N'_o for these channels are not very well measured.

Comparisons

Different Configurations

The noise obtained using the calibration method for the different configurations can be compared [figure 33 and table X].

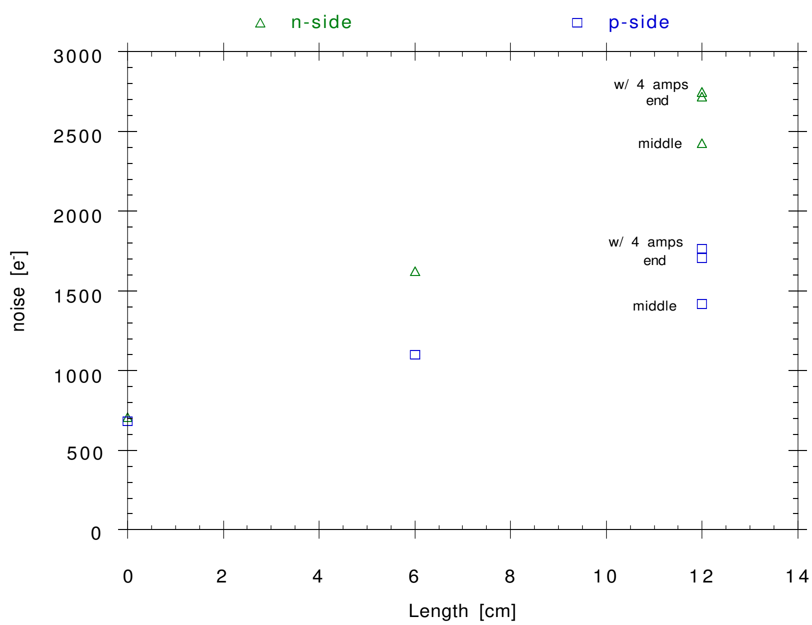

Figure 33 - Noise obtained with the calibration method for the different configurations.

Table X - Noise for 0, 6 and 12cm strips for the calibration method and different configurations.

	noise [fC]	
	n-side	p-side
0cm	706.25	681.25
6cm	1625.0	1100.0
12cm w/ 4 neighboring amplifiers	2746.6	1766.5
12cm - middle	2428.2	1417.0
12cm - end	2718.7	1706.3

We have converted the noise in fC into the noise in electrons[20].

Looking at figure 33 one can see that, in general, the noise for a strip scales with the length of the strip. The graph shows the noise scaling linearly with length of the strip, but we must be careful in making comparisons. The 6cm strips have all of their neighbors connected to an amplifier, where the 12cm strips have their nearest neighbors connected to an amplifier and their next nearest neighbors floating. This poses a problem since we do not know the contribution to the noise from the next nearest neighbors if they are floating. We do know that the contribution from the next nearest neighbors is small, compared to the contribution from the nearest neighbors, if they are connected to an amplifier. We would like to assume that the contribution is small also if the next nearest neighbors are floating, but we have not shown this.

The noise for the 12cm strips with 4 neighboring amplifiers has the highest noise of all the 12cm configurations. This is possibly due to the contribution of the two extra neighbors, although the difference in noise between this configuration and the 12cm strips connected at the end of the detector is within our error [5%]. The 20% difference in noise for the 12cm - end and 12cm - middle configurations is significant. These two configurations both have floating strips and so are directly comparable. The noise is lower for a 12cm strip connected at the middle than for one connected at the end because the resistance for the 12cm - middle configuration is lower than for the 12cm - end configuration.

Occupancy Method - Gaussian and Complementary Error Function

The data for a 0, 6 and 12cm strip for the n and p-side with both the gaussian approximation and complementary error function fit are shown in figure 34 to 39.

---

[20] This is easily accomplished by dividing the noise in fC by 1.602×10^{-4} fC/e^-.

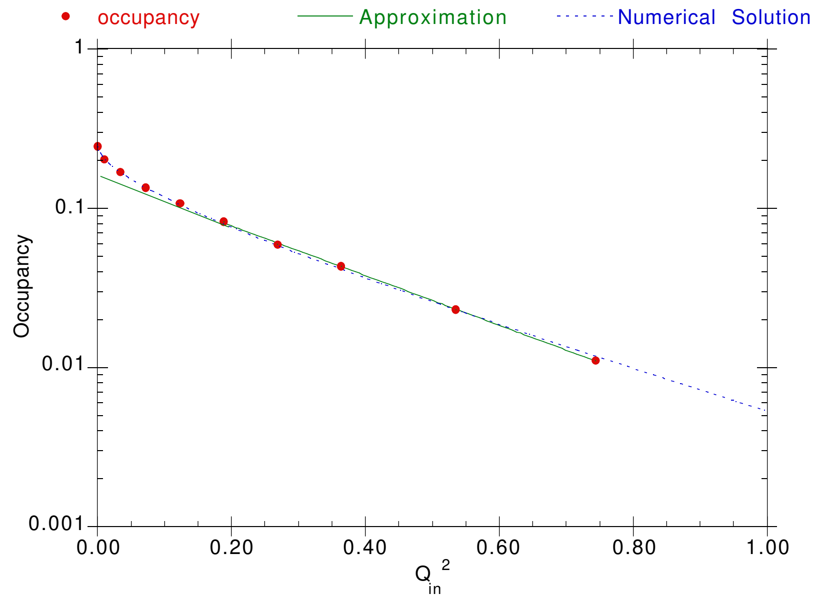

Figure 34 - Data for a n-side 12cm-end strip with fits for the gaussian approximation and the complementary error function.

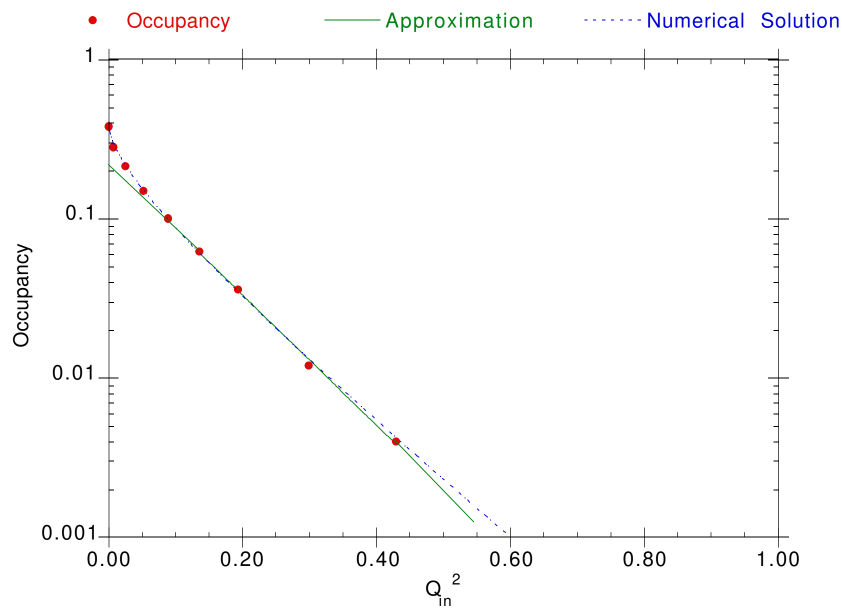

Figure 35 - Data for a p-side 12cm-end strip with fits for the gaussian approximation and the complementary error function.

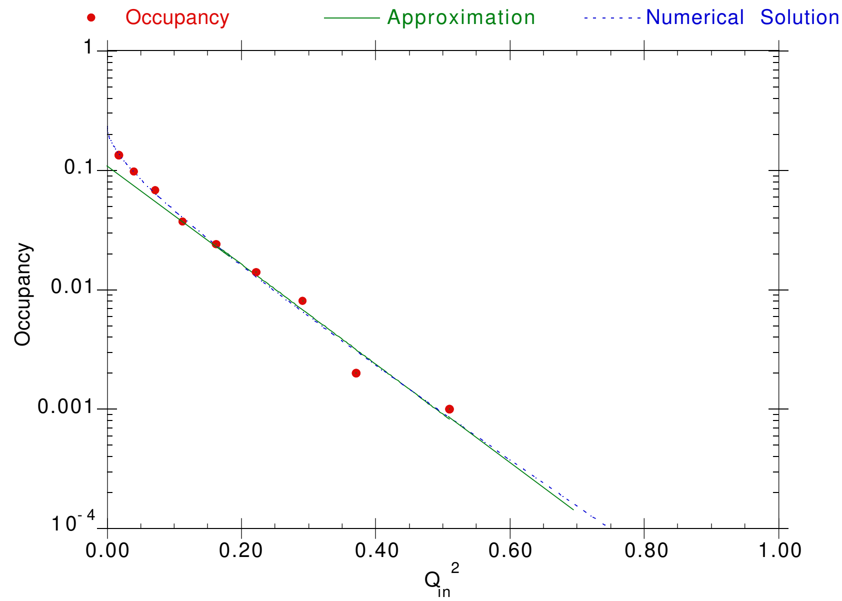

Figure 36 - Data for a n-side 6cm strip with fits for the gaussian approximation and the complementary error function.

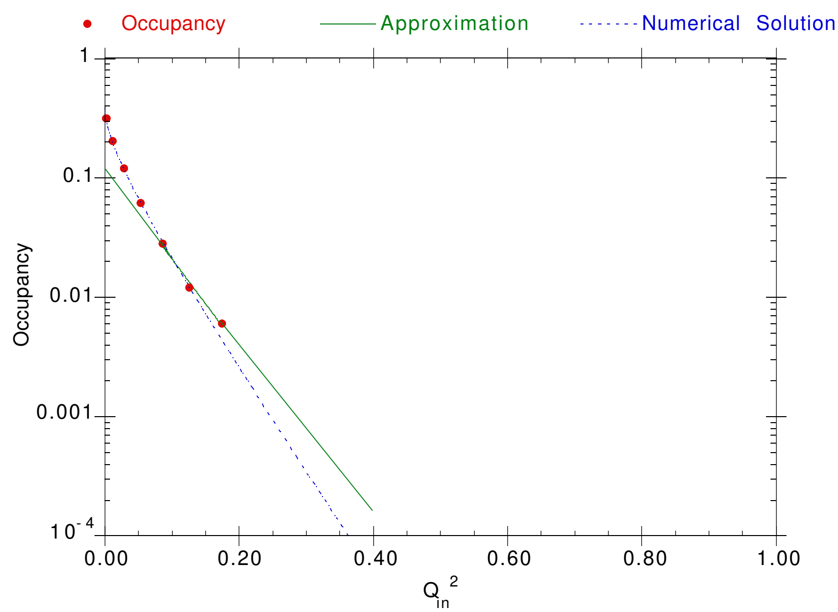

Figure 37 - Data for a p-side 6cm strip with fits for the gaussian approximation and the complementary error function.

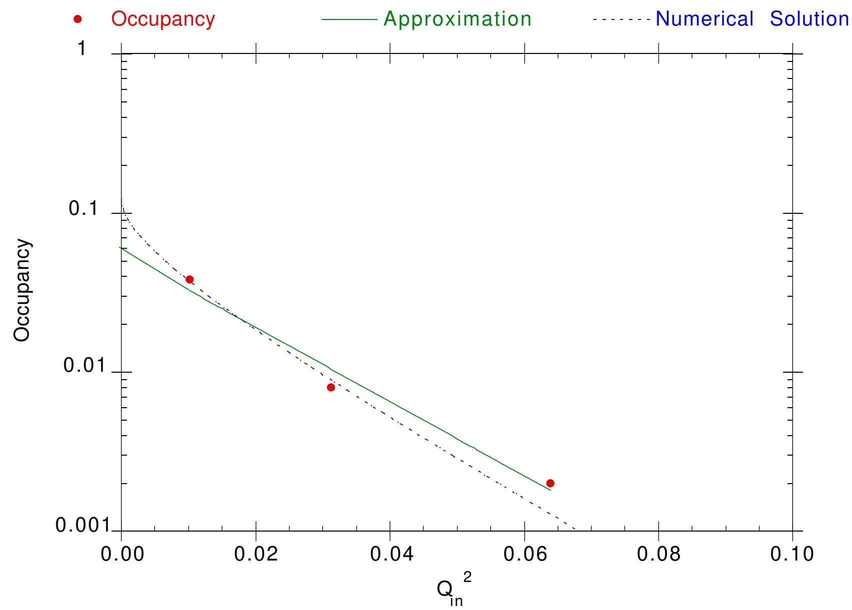

Figure 38 - Data for a n-side 0cm strip with fits for the gaussian approximation and the complementary error function.

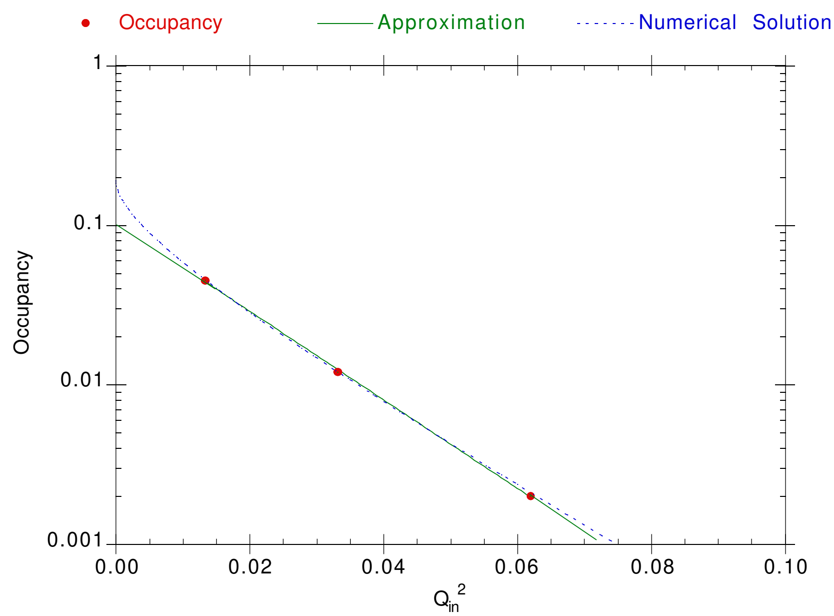

Figure 39 - Data for a p-side 0cm strip with fits for the gaussian approximation and the complementary error function.

The noise obtained for the occupancy method using the gaussian approximation and the complementary error function fit can be compared [figure 40 and table XI].

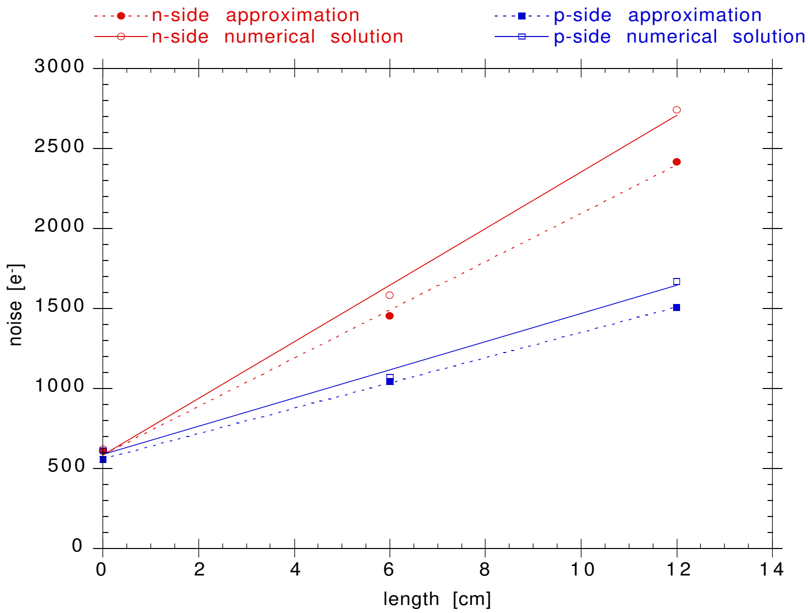

Figure 40 - Noise vs. length for the occupancy method using the gaussian approximation and the complementary error function fit.

Table XI - Noise for 0, 6 and 12cm - end strips for the occupancy method using the gaussian approximation and the complementary error function fit

		noise [e⁻]	
		Gaussian Approximation	Complementary Error Function
0cm strip	n-side	606.25	617.98
	p-side	556.25	611.74
6cm strip	n-side	1456.25	1579.28
	p-side	1043.75	1067.42
12 cm strip - end	n-side	2362.50	2710.32
	p-side	1506.25	1666.67

Here, again, we present the noise in electrons instead of fC.

The noise obtained using the gaussian fit is on average 10% lower than the noise obtained using the complementary error function fit. When using the complementary error function we obtain a fit that seems to match the data well [see figures 34-39]. But, we are fitting the data in a range where the correct behavior of the response curve is not known. When fitting the data to the gaussian only the points for higher input charge are used; the sharp rise for small input charge is not included, so the data is fit in a range where we do have experimental points for the response curve.

Assuming that a complementary error function describes the noise distribution perfectly, a theoretical curve can be fit with a gaussian and the sigma obtained from the fit can be compared to the theoretical sigma. It is apparent from figure 21 that depending in which range the complementary error function is fit, a different slope and therefore sigma will be found. We are interested in comparing this result with the those obtained from the gaussian fit to the data. Therefore, the range for which the data was fit using the gaussian approximation can be used to fit the complementary error function. This range is $(Q_{in}/\text{sigma})^2$ between one and seven. We find that, in this range, the slope of the gaussian that is fit to the theoretical complementary error function is 10% less than the theoretical value. Therefore the gaussian approximation is underestimating the noise by 10%.

This explains the on average 10% difference between the noise for the gaussian and complementary error function fit, and shows that the fit of the data to the complementary error function gives the correct figure for the noise.

Occupancy Method vs. Calibration Method

The results for the occupancy method, with the gaussian and with the complementary error function fit can be compared to the results for the calibration method.

Figure 41 and table XII shows the results for the gaussian fit and the calibration method.

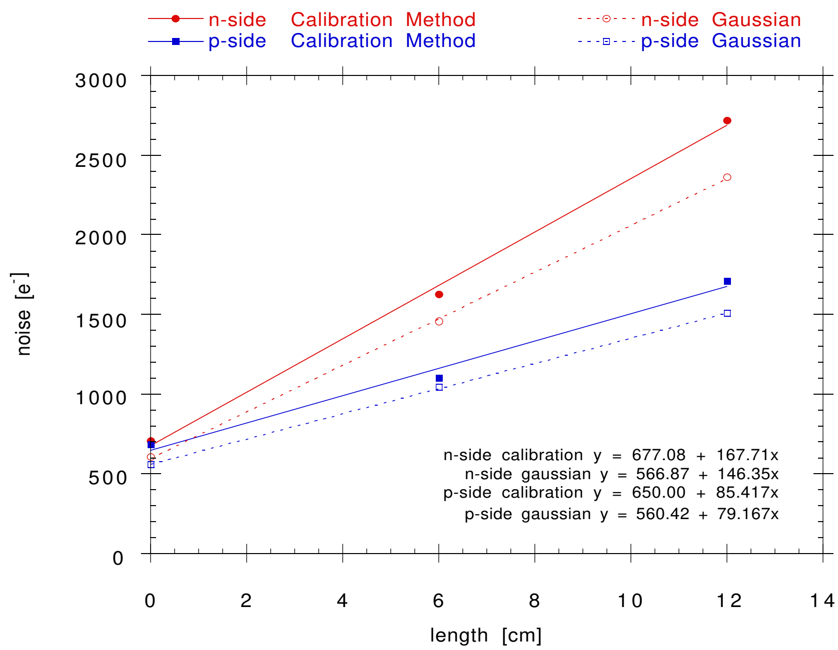

Figure 41 - Comparison of the occupancy method using the gaussian fit and the calibration method.

Figure 42 and table XII shows the results for the complementary error function fit and the calibration method.

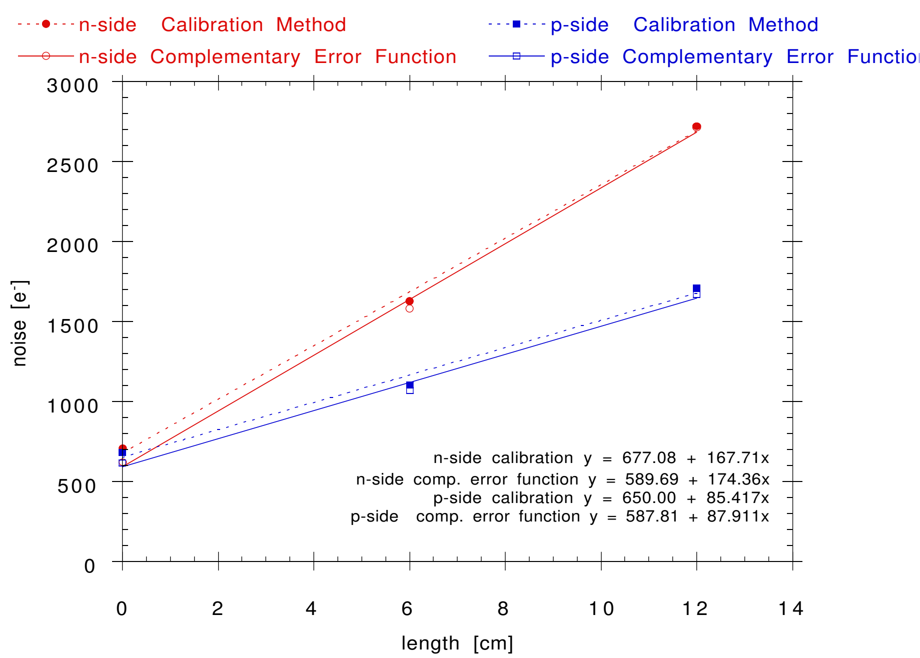

Figure 42 - Comparison of the occupancy method using the complementary error function fit and the calibration method.

Table XII - Noise for 0, 6 and 12cm - end strips for the occupancy and calibration method.

		noise [e^-]		
			Occupancy Method	
		Calibration Method	Gaussian	Comp. Error Function
0cm strip	n-side	706.25	606.25	617.98
	p-side	681.25	556.25	611.74
6cm strip	n-side	1625.00	1456.25	1579.28
	p-side	1100.00	1043.75	1067.42
12 cm strip - end	n-side	2718.75	2362.50	2710.32
	p-side	1706.25	1506.25	1666.67

We also see an average of 10% difference in the noise between the gaussian and the calibration method. Following the argument presented above we can conclude that the noise found using the calibration method is correct.

The noise obtained for the calibration method and the noise obtained using the complementary error function fit for the occupancy method agree within an average of 5%.

Although, as mentioned before, the noise for 12cm - end strips is not directly comparable with the 0 and 6cm strips because of its floating next nearest neighbors, we can still draw some conclusions from the linearity observed in figure 41 and 42. If we assume that the noise is described by equation 1, we can calculate how well the data matches the theoretical constants A and B.

From equation 1 we have: $y = A + BC$ where $A = 600e^-$ and $B = 32\ e^-/pF$. In figure 41 and 42 a linear fit for the data gives us the equation $y = A + Dx$ where x is the length of the strip. The values of A for the calibration method and for the occupancy method are reasonably close to the theoretical value.

Comparing the two equations, we know Dx must equal BC and from this we can solve for an experimental value for B and compare it to the theoretical value. The capacitance for a n-side strip is 2pF/cm and for a p-side strip it is 1.2pF/cm [21]. The calculations for B are presented in table XIII.

Table XIII - The factor B as determined from the linear fit of noise vs. length.

	B [e^-/pF]	
	n-side	p-side
Calibration Method	84	71
Gaussian Approximation	73	66
Complementary Error Function	87	73

One can see that the values for B in table XIII are much larger than the theoretical value of 32e^-. This shows us that there is a large contribution to the noise from the neighboring amplifiers and the resistance.

The value of B for the calibration method and the complementary error function fit are approximately the same which confirms the fact that they both provide the correct results for the noise. Again, we see that the values for the gaussian approximation are 10% less than the others.

V. CONCLUSION

We can draw some conclusions from the data presented here.

We have been able to determine noise, using three different methods to an accuracy of 5%.

We have found that the calibration method and the occupancy method when the complementary error function is used to fit the data provides a reliable result for the noise. The occupancy method, when the gaussian approximation is used to fit the data, gives a value for the noise which is 10% too low.

The occupancy method provides a more real measurement of the noise that is present during a collider experiment. In an experiment, the detectors are sitting, waiting for a particle to pass through and provide a signal. For the

---

21 Barberis, p. 92 - 94.

occupancy method we are also just sitting, waiting and collecting noise; we are not introducing anything artificial to an experimental situation. But, for the occupancy method, in order to convert the threshold voltage into an input charge, the response curve generated by the calibration method must be used.

When the gaussian is used to determine the noise for the occupancy method the data is fit in a range for which the response curve is experimentally known. But, the gaussian fit totally ignores the behavior of the data for small input charges.

When the complementary error function fit is used to determine the noise the sharp rise in the occupancy for small input charges is taken into account. For this method the behavior of the data better described, but we are in a region where the response curve is not experimentally known.

The noise measurements taken with material placed on top of the detector did provide conclusive results. In order to see an effect the material would have to be very close [within 10μm] to the detector. For all practical purposes the material placed on the detector would be far enough away so that any effect is negligible. This has positive implications for the design of new detector hybrids which are made of Kapton or alumina, hold all the readout electronics, but sit directly on top of the detector. A detector board like this is now being designed for the ATLAS experiment at CERN.

We have attempted to determine how noise scales with the length of the detector. Due to bonding difficulties, for certain configurations, some strips have been left floating. We do not know how to calculate what effect these floating strips have on the capacitance and therefore the noise of other strips. This problem along with larger statistical and systematic errors than were expected have left many of our results inconclusive. To get around the problem posed by floating strips a means of grounding the disconnected strips so as to avoid clock pickup needs to be investigated. With grounded neighbors the change in capacitance and therefore in noise can be calculated and predicted.

There are many new measurements that we would like to make to work around some of the problems we discovered and to investigate new properties of the detector.

A measurement for 6cm strips with floating next nearest neighbors will be made to compare with the results for 12cm strips with floating next nearest neighbors. We would then have noise measurements for 0cm, 6cm and 12cm strips which are comparable. From this we could start to determine how noise scales with the length of the detector.

In order to find the contribution of floating next nearest neighbors measurements for 6cm strips with floating nearest neighbors can be compared to measurements of 6cm strips with neighbors connected to amplifiers.

We would also like to investigate how noise scales with the resistance of the detector. We have two detectors, one with a strip resistance[22] of 50 ohms/cm and one with a resistance of 90 ohms/cm. Noise measurements for the same configurations on both of the detectors will be made and compared.

We also will do SPICE simulations for all of these configurations and compare that output to the measurements. Using simulations theories can be tested and new characteristics of the detector[which is the resistance of the detector that was used for the measurements presented in this paper] can be discovered and understood.

[22] The detector that was used for the measurements presented in this paper has a strip resistance of 50 ohms/cm.

References

E. Barberis et al., “Capacitances in silicon microstrip detectors.” Nuclear Instruments and Methods in Physics Research A 342 (1994) 90-95.

Joel DeWitt, "A Pipeline and Bus Interface Chip for Silicon Strip Detector Read-Out," SCIPP 93/37.

Robert Johnson, "Capacitance of Detectors Covered by Dielectrics," U.C. Santa Cruz, March 6, 1995 (unpublished paper).

A. M. Litke and A. S. Schwarz, “The Silicon Microstrip Detector," Scientific American, May 1995.

John Nibarger, "Capacitance Measurement Techniques for Silicon Microstrip Detectors", U.C. Santa Cruz, Bachelor of Science in Physics Thesis.

Kimberly J. Noble, “A Correction For The Calculation Of The Input Charge During Calibration Runs,” U.C. Santa Cruz, March 28, 1995 (unpublished paper)

S.O. Rice, Bell Systems Technical Journal 23, 282 (1944).

Spencer et al., "A Fast Shaping Low Power Amplifier-Comparator Integrated Circuit for Silicon Strip Detectors," SCIPP 94/32.

Helmuth Spieler, “Power Requirements for Front-End Electronics in the Silicon Tracker,” Lawrence Berkeley Laboratory, 6 September 1991.

Appendix A - Input Charge Corrections[23]

In order to determine the charge presented to the input of the amplifier for different voltage setting of the DAC we made measurements of the pulse height on the detector board for a given voltage setting. The results were fit to a linear function of the form

$$V_m = AV_{cal} + B \qquad [15]$$

where V_m is the measured voltage for a DAC setting of V_{cal}. We found that the values for A and B were dependent on the chip type, calibration line, fan-out board and the number of detector boards connected. The measurements presented in this paper were taken on strips from calibration line 2 and with only one detector board connected to the set up. Table XIV shows the values for A and B for both the n and p-side for this situation.

Table XIV - Values of A and B for calibration line 2 when one detector board is connected.

chip type	A [mV/V]	B [mV]
n	63.15	-38.21
p	63.09	-38.50

Using these values for A and B we can calculate the input charge.

$$Q_{in} = \frac{84}{3 \cdot 1000}\left[AV_{cal} + B\right] \qquad [16]$$

where Q_{in} is the input charge in fC; 84 is the value of the calibration capacitor in fF; 1/3 is due to the fact that a voltage divider is limiting the signal to the capacitor and 1/1000 assures that our value for Q_{in} is in fC.

The value for Q_{in} calculated from equation 16 is the actual charge that is injected by the calibration capacitors. But there is another effect to consider. The calibration pulse is delivered to 16 channels at one time which reduces the charge seen at the input to the amplifier for each strip. Therefore, the best estimate of the input charge that the amplifier for each of the 16 strips sees is

[23] For a more detailed discussion see Noble [1995].

$$Q_{effective} = \frac{Q_{in}}{1 + \exp[-m_1(Q_{in} + m_2)]} \qquad [17]$$

where Q_{in} is calculated from equation 16, m_1 = 0.29 and m_2 = 5.30.

$Q_{effective}$ is the value for the input charge that is used in all of the data analysis calculations.